CHAPTER SEVENTEEN

The MOD-QM/MM Method: Applications to Studies of Photosystem II and DNA G-Quadruplexes

M. Askerka*, J. Ho*,[1], E.R. Batista†, J.A. Gascón‡, V.S. Batista*,[2]
*Yale University, New Haven, CT, United States
†Los Alamos National Laboratory, Los Alamos, NM, United States
‡University of Connecticut, Storrs, CT, United States
[2]Corresponding author: e-mail address: victor.batista@yale.edu

Contents

Abstract

Quantum mechanics/molecular mechanics (QM/MM) hybrid methods are currently the most powerful computational tools for studies of structure/function relations and catalytic sites embedded in macrobiomolecules (eg, proteins and nucleic acids). QM/MM methodologies are highly efficient since they implement quantum chemistry methods for modeling only the portion of the system involving bond-breaking/forming processes (QM layer), as influenced by the surrounding molecular environment described in terms of molecular mechanics force fields (MM layer). Some of the limitations of QM/MM methods when polarization effects are not explicitly considered include the approximate treatment of electrostatic interactions between QM and MM layers. Here, we review recent advances in the development of computational protocols that allow for rigorous modeling of electrostatic interactions in biomacromolecules and structural

[1] Institute of High Performance Computing, 1 Fusionopolis Way, #16-16 Connexis North, Singapore 138632.

Methods in Enzymology, Volume 577
ISSN 0076-6879
http://dx.doi.org/10.1016/bs.mie.2016.05.021

refinement, beyond the common limitations of QM/MM hybrid methods. We focus on photosystem II (PSII) with emphasis on the description of the oxygen-evolving complex (OEC) and its high-resolution extended X-ray absorption fine structure spectra (EXAFS) in conjunction with Monte Carlo structural refinement. Furthermore, we review QM/MM structural refinement studies of DNA G4 quadruplexes with embedded monovalent cations and direct comparisons to NMR data.

1. INTRODUCTION

The development of computer architectures and efficient algorithms has allowed computational chemistry to establish itself as a powerful and valuable tool for general purpose applications, including a wide range of structural and mechanistic studies of large biomolecular systems (eg, proteins and nucleic acids). In particular, hybrid quantum mechanics/molecular mechanics (QM/MM) methods have become available in popular software packages and are routinely applied in studies of catalytic complexes embedded in enzymatic macromolecular structures (Bakowies & Thiel, 1996; Dapprich, Komaromi, Byun, Morokuma, & Frisch, 1999; Field, Bash, & Karplus, 1990; Humbel, Sieber, & Morokuma, 1996; Luber et al., 2011; Maseras & Morokuma, 1995; Murphy, Philipp, & Friesner, 2000b; Pal et al., 2013; Philipp & Friesner, 1999; Shoji, Isobe, & Yamaguchi, 2015a; Shoji et al., 2015b; Singh & Kollman, 1986; Svensson et al., 1996; Vreven & Morokuma, 2000a, 2000b; Warshel & Levitt, 1976). QM/MM methods significantly expand the scope of quantum mechanical calculations to much larger systems by limiting the quantum mechanical description (typically based on density functional theory (DFT)) to a subsystem where chemical reactivity is localized (QM layer), while the "spectator" region is usually treated with an inexpensive model chemistry such as classical molecular mechanics force fields, or a lower level of electronic structure theory (eg, semiempirical methods). This partitioning scheme ensures highly efficient, yet accurate, modeling of electrostatic interactions as exploited by the Moving-Domain QM/MM (MOD-QM/MM) methodology (Gascon, Leung, Batista, & Batista, 2006; Ho et al., 2014; Menikarachchi & Gascon, 2008; Sandberg, Rudnitskaya, & Gascón, 2012) and the studies of the oxygen-evolving complex (OEC) of photosystem II (PSII) reviewed in this chapter.

Technical differences between the various QM/MM methods concern whether the energy is evaluated according to additive or subtractive schemes, and whether the boundaries between QM and MM layers are

treated with link atoms, pseudopotentials, or localized bond orbitals (Senn & Thiel, 2009; van der Kamp & Mulholland, 2013). Other differences include the level of quantum chemistry and MM force field and different approaches for the description of electrostatic interactions between the QM and MM layers (eg, mechanical embedding, electronic embedding, and polarized embedding schemes). In particular, the mechanical embedding approach couples in vacuo QM electronic densities with point charges in the MM layer, as described by classical electrostatic interactions. In the electronic embedding approach, the atom-centered point charges in the MM layer can polarize the QM electronic density. Finally, higher-level corrections to include the mutual polarization between the MM and QM layers can be included in the polarized embedding scheme (Devries et al., 1995; Eichler, Kolmel, & Sauer, 1997; Gao & Xia, 1992; Thompson, 1996; Vreven, Mennucci, da Silva, Morokuma, & Tomasi, 2001), and in the MOD-QM/MM scheme (Gascon, Leung, et al., 2006; Ho et al., 2014; Menikarachchi & Gascon, 2008).

The MOD-QM/MM method partitions the system into molecular domains and obtains the geometry and electrostatic properties of the whole system from an iterative self-consistent treatment of the constituent molecular domains (Gascon, Leung, et al., 2006; Ho et al., 2014; Menikarachchi & Gascon, 2008; Sandberg et al., 2012). Self-consistently optimized structures and electrostatic potential (ESP) atomic charges are obtained for each domain modeled as a QM layer polarized by the distribution of atomic charges in the surrounding fragments. The resulting computational task scales linearly with the size of the system, bypassing the exponential demand of memory and computational resources typically required by "brute-force" full QM calculations. Computations for several benchmark systems that allow for full QM calculations have shown that the MOD-QM/MM method produces ab initio quality structures and ESPs in quantitative agreement with full QM results (Gascon, Leung, et al., 2006; Ho et al., 2014; Menikarachchi & Gascon, 2008; Sandberg et al., 2012). The work reviewed in this chapter illustrates the MOD-QM/MM method as applied to the description of macromolecules of biological interest, including PSII and DNA quadruplexes, in conjunction with structural refinement based on simulations of X-ray absorption spectra and direct comparisons with experimental data.

The key aspect of MOD-QM/MM is the description of polarization effects in the MM layer of QM/MM calculations. In that respect, a number of methods were previously proposed (Mayhall & Raghavachari, 2012;

Saha & Raghavachari, 2015). One of them includes a standard atomic dipole description where dipole moments are induced in each atom of the MM layer, defined as the product of the atomic polarizability and the electric field at the position of the atom (Houjou, Inoue, & Sakurai, 2001; Illingworth et al., 2006; Thompson, 1996; Thompson & Schenter, 1995; Warshel, 1976). Atomic polarizabilities are therefore required as input parameters. The approach has been implemented at the "ab initio" level in quantum chemistry packages such as GAMESS (Schmidt et al., 1993) and Q-CHEM (Shao et al., 2015) where it is called an "effective fragment potential" method (Chen & Gordon, 1996; Day et al., 1996; Gordon et al., 2001). The polarization of the fragments is described by standard distributed multipoles, using atomic polarizabilities obtained in preliminary ab initio calculations as input parameters. Another related approach is the explicit polarization (X-Pol) method, which is an approximate fragment-based molecular orbital method. This approach incorporates many-body polarization at a cost that scales linearly with the number of fragments but must be augmented with empirical Lennard-Jones potentials (Gao, 1998; Xie, Orozco, Truhlar, & Gao, 2009).

Polarization effects can be accounted for at the MM level by using polarizable force fields (Banks et al., 1999; Bernardo, Ding, Kroghjespersen, & Levy, 1994; Burnham & Xantheas, 2002; Corongiu, 1992; Halgren & Damm, 2001; Huang, Lopes, Roux, & MacKerell, 2014; Maple et al., 2005; Palmo, Mannfors, Mirkin, & Krimm, 2003; Ren & Ponder, 2003; Schworer et al., 2013; Stern et al., 1999; Stern, Rittner, Berne, & Friesner, 2001; Vanommeslaeghe & MacKerell, 2015; Yu, Hansson, & van Gunsteren, 2003), although such methods are computationally expensive. One of the early classical methods to describe polarization effects has been the "fluctuating charge model," studied by Rappe and Goddard (Rappe & Goddard, 1991), Berne (Bader & Berne, 1996; New & Berne, 1995; Rick & Berne, 1996; Rick, Stuart, Bader, & Berne, 1995; Rick, Stuart, & Berne, 1994; Stuart & Berne, 1996), Parr and Yang (Parr & Yang, 1989), Friesner and Berne (Stern et al., 2001), and Field (Field, 1997). In this model, the system is broken down into fragments; whereas the total charge of the fragment is conserved, the charges on the atoms are calculated self-consistently through minimizing the total energy of the system with respect to the atomic charges. This self-consistent procedure leads to the charges, for which the partial derivatives of the total energy E with respect to the atomic charges—electronegativities—are equal. Similar approaches include the chemical potential equalization proposed

by York and Yang (York, 1995; York & Yang, 1996) and the Drude oscillator models implemented by Voth (Lobaugh & Voth, 1994), Chandler (Thompson, Schweizer, & Chandler, 1982), Cao and Berne (Cao & Berne, 1992), and Sprik and Klein (Sprik & Klein, 1988).

Semiempirical models, based on the equalization of atomic electronegativities (Borgis & Staib, 1995; Field, 1997; Gao, 1997), obtain the self-consistent density matrices of the constituent fragments by neglecting the off-diagonal elements associated with atoms of different fragments. The interaction between the fragments can be added back by including Lennard-Jones potential term as well as electrostatic interactions based on Mulliken charges (Field, 1997; Gao, 1997). The Mulliken charges can be then improved by rescaling, using empirical parameters obtained from comparisons of the computed and experimental properties of the system (Gao, 1997). The charges can be also calculated using a semiempirical charge model (CM), developed by Cramer and Truhlar (Storer, Giesen, Cramer, & Truhlar, 1995). However, the charges cannot be improved to reproduce ab initio quality ESPs, as in the MOD-QM/MM method since they would be too small and would require empirical scaling (Field, 1997; Gao, 1997).

Semiempirical fluctuating CMs also differ from MOD-QM/MM in the treatment of the boundaries between QM and MM layers. MOD-QM/MM was specifically designed to model ESPs of extended systems (eg, proteins, RNA, DNA) where it is necessary to cut covalent bonds to define the boundaries between QM and MM layers. When combined with accurate calculations of ESP atomic charges, the MOD-QM/MM method allows one to obtain ab initio quality ESPs and refined structures of extended systems.

The MOD-QM/MM approach usually converges within a few iterations of self-consistent calculations of polarized charges and optimized geometries of the constituent domains, and therefore has convergence properties similar to those of "linear scaling" techniques where the whole system is treated at the QM level (Babu & Gadre, 2003; Baldwin, Kampf, & Pecoraro, 1993; Burant, Scuseria, & Frisch, 1996; Daniels & Scuseria, 1999; Greengard & Rokhlin, 1987; Li, Nunes, & Vanderbilt, 1993; Schwegler & Challacombe, 1996; Strain, Scuseria, & Frisch, 1996; Stratmann, Burant, Scuseria, & Frisch, 1997; Stratmann, Scuseria, & Frisch, 1996; Strout & Scuseria, 1995; White & Headgordon, 1994; White, Johnson, Gill, & HeadGordon, 1996). In such linear scaling methods, the high computational cost is avoided by neglecting the two electron integrals between orbitals that are situated at long distances from each other, leading to sparse Fock matrices. Full diagonalization

is circumvented and the correlation energy is computed in a less expensive way (Ko et al., 2003; Saebo & Pulay, 1993), or by using localized orbitals (Subotnik & Head-Gordon, 2005). Another linear scaling method is the "divide-and-conquer" technique, developed by Yang and coworkers (Lee, York, & Yang, 1996; Yang, 1991; Yang & Lee, 1995). Such a method divides the density matrix into fragments that are treated by conventional quantum chemistry techniques to ultimately obtain the properties of the whole system. Later, Merz and coworkers developed a semiempirical version of divide-and-conquer (Dixon & Merz, 1996, 1997; Ermolaeva, van der Vaart, & Merz, 1999), Exner and Mezey proposed the adjustable density-matrix assembler approach (Exner & Mezey, 2002, 2003, 2004), Zhang and coworkers developed the molecular fractionation with conjugated caps approach (Gao, Zhang, Zhang, & Zhang, 2004; Kurisu, Zhang, Smith, & Cramer, 2003; Mei, Zhang, & Zhang, 2005; Zhang, Xiang, & Zhang, 2003; Zhang & Zhang, 2003), Gadre and coworkers developed the molecular tailoring approach (Babu & Gadre, 2003; Babu, Ganesh, Gadre, & Ghermani, 2004; Gadre, Shirsat, & Limaye, 1994), Kitaura and coworkers proposed the fragment molecular-orbital FMO method (Fedorov & Kitaura, 2004a, 2004b; Kitaura, Ikeo, Asada, Nakano, & Uebayasi, 1999; Kitaura, Sugiki, Nakano, Komeiji, & Uebayasi, 2001), Li and coworkers proposed the localized molecular-orbital assembler approach (Li & Li, 2005; Li, Li, & Fang, 2005), Mayhall and Raghavachari proposed the multilayer molecules-in-molecules method that is similar in spirit to the ONIOM approach (Mayhall & Raghavachari, 2011) (vide infra), while Collins and Bettens introduced the combined and systematic fragmentation approach (Collins, Cvitkovic, & Bettens, 2014).

The MOD-QM/MM approach does not have any kind of limitation with regard to the level of quantum chemistry applied to describe the QM layer. Typically, it has been implemented by using DFT, which allows for an efficient description of electron correlation at the computational cost of single-determinant calculations. MOD-QM/MM with DFT has been successfully applied to PSII and other biological systems (Gascon, Leung, Batista, & Batista, 2006; Gascon, Sproviero, & Batista, 2006; Gascon, Sproviero, McEvoy, Brudvig, & Batista, 2008; Menikarachchi & Gascon, 2008; Sandberg et al., 2012; Sproviero, Gascon, McEvoy, Brudvig, & Batista, 2006a, 2006b, 2007, 2008a, 2008b, 2008c, 2008d). This includes modeling charge redistribution, polarization effects and changes in the ligation scheme of metal centers induced by oxidation state transitions, and bond breaking and forming processes associated with chemical reactivity

and proton transfer. The resulting MOD-QM/MM model systems have allowed for direct comparison with high-resolution spectroscopic data, including FTIR, NMR, extended X-ray absorption fine structure spectra (EXAFS), and EPR spectroscopy (Sproviero et al., 2007; Sproviero, Gascon, et al., 2008a, 2008b, 2008c, 2008d, 2008b).

This chapter reviews the MOD-QM/MM as a rigorous yet practical methodology suited to study a wide range of enzymes and biological systems, including DNA, RNA, and proteins with catalytic sites beyond the capabilities of molecular mechanics force fields. The presentation is organized as follows. First, we review the QM/MM methodology, including a detailed discussion of its implementation to metalloenzymes and DNA. Then, we review the post-QM/MM refinement scheme based on simulations of X-ray absorption spectra and direct comparisons with experimental measurements. The applications review benchmark studies, illustrating the capabilities of the MOD-QM/MM methodology and the post-QM/MM analysis of model structures through direct comparisons with NMR and EXAFS spectroscopic data.

2. METHODS

2.1 QM/MM Methodology

The MOD-QM/MM method is a general approach that can be applied in conjunction with any electronic embedding QM/MM methods (Chung, Hirao, Li, & Morokuma, 2012; Gascon, Leung, et al., 2006; Menikarachchi & Gascon, 2008; Sproviero, Gascon, et al., 2008b; Vreven et al., 2006). It has been implemented in the ONIOM (Chung et al., 2012; Vreven et al., 2006) electronic embedding method in the Gaussian program (Frisch et al., 2004). The ONIOM method is a subtractive QM/MM approach. When implemented in term of two layers, the whole system is partitioned into a "high-level" layer generally treated with QM methods and a "low-level" layer, described by MM force fields (Fig. 1). The total energy is given by the following extrapolation,

$$E = E^{\mathrm{MM,high+low}} + E^{\mathrm{QM,high}} - E^{\mathrm{MM,high}} \tag{1}$$

where $E^{\mathrm{MM,high+low}}$ is the energy of the full system computed at the molecular mechanics level of theory, while $E^{\mathrm{QM,high}}$ and $E^{\mathrm{MM,high}}$ are the energies of the high-level layer calculated by using QM and MM levels of theory, respectively. In this extrapolation scheme, electrostatic interactions

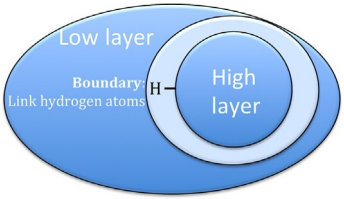

Fig. 1 QM/MM fragmentation of the system into a reduced QM (high) layer and the surrounding molecular environment described as an MM (low) layer.

computed at the MM level in $E^{\mathrm{MM,high}}$ and $E^{\mathrm{MM,high+low}}$ cancel, therefore, giving a quantum mechanical description of polarization of the high layer due to the electrostatic influence of the surrounding environment. However, when implemented with standard nonpolarizable force fields based on distributions of single point atomic charges (eg, Amber (Cornell et al., 1995), CHARMM (Vanommeslaeghe & MacKerell, 2015)), the method does not include the self-consistent polarization of the MM layer due to the distribution of charge in the QM layer. Such a polarization effect often corresponds to small corrections of single point atomic charges of about 10–15%. However, adding all of the corrections over the whole interface between the QM and MM layers often amounts to significant energy corrections of 10–15 kcal mol^{-1}. Neglecting such corrections during energy minimization, thus, can lead to structural rearrangement artifacts in both of the QM and MM layers. The MOD-QM/MM approach is a simple methodology for addressing these important corrections.

2.2 MOD-QM/MM Method

In the MOD-QM/MM method, the system is partitioned into n molecular domains using a simple space-domain decomposition scheme (Gascon, Leung, et al., 2006; Ho et al., 2014; Menikarachchi & Gascon, 2008). A two-layer QM/MM scheme is used to optimize the geometry of each molecular domain and to compute the electrostatic potential (RESP) atomic charges of each fragment as influenced by the surrounding molecular environment. Mutual polarization interactions between the constituent molecular domains are thus included and the whole cycle of QM/MM calculations is iterated several times until a self-consistent geometry and point-charge model of the ESP are obtained.

Fig. 2 illustrates the application of the MOD-QM/MM method on a guanine G-DNA quadruplex, where each domain corresponds to one of the guanine nucleotides. The self-consistent solution is usually obtained within a few (four to five) iterations, which makes the computational cost

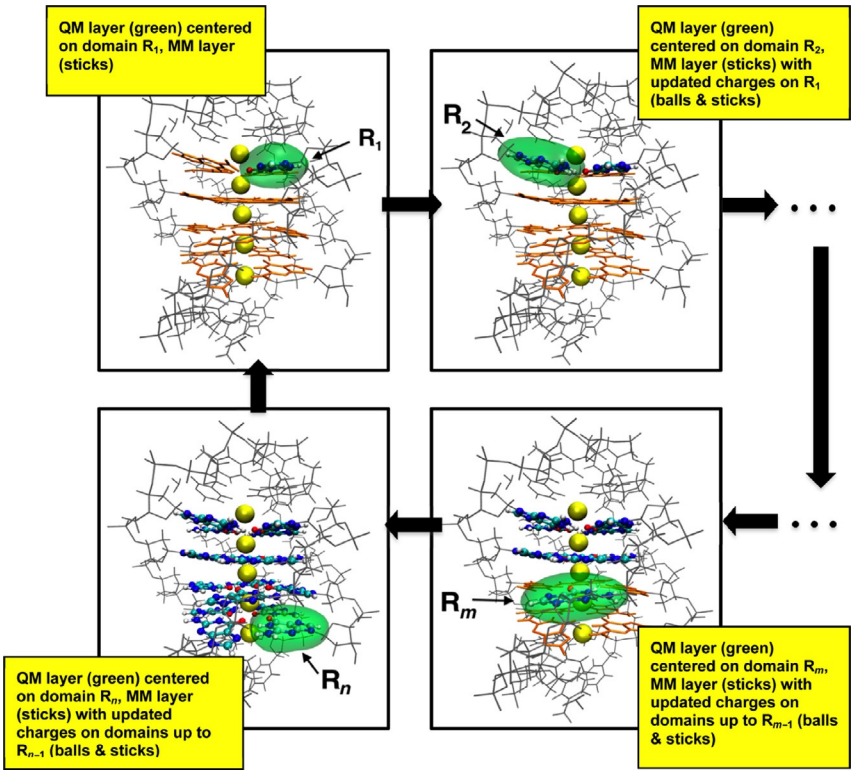

Fig. 2 MOD-QM/MM iterative cycle of QM/MM calculations with QM layers (in *green* (*gray* in the print version)) defined on individual molecular domains along the different steps of the cycle (Gascon, Leung, et al., 2006). *Balls* and *sticks* represent molecular domains with ESP atomic charges updated in previous steps of the cycle. *Ho, J., Newcomer, M.B., Ragain, C.M., Gascon, J.A., Batista, E.R., Loria, J.P., & Batista, V.S. (2014). The MoD-QM/MM structural refinement method: Characterization of hydrogen bonding in the Oxytricha nova G-quadruplex.* Journal of Chemical Theory and Computation, 10, *5125–5135. Copyright American Chemical Society 2014.*

scale linearly with the system size. This makes MOD-QM/MM much more applicable when compared to the quantum-chemical treatment of the complete system.

The atomic charges obtained by the MOD-QM/MM iterative procedure typically correct the charges of popular molecular mechanics force fields (Cornell et al., 1995; Dykstra, 1993) by only 10–20%. As mentioned before, however, these small corrections across multiple domains can amount to a significant change in energy (10–15 kcal/mol). Those corrections are comparable to the energetics of changes in protonation states, hydrogen-bonding pattern, or oxidation state transitions of redox-active

cofactors. Therefore, it is important to properly account for electrostatic interactions that could otherwise lead to artifact structural rearrangements across multiple domains over the entire QM/MM interface.

Ab initio quality molecular electrostatic potentials are obtained from the updated distribution of atomic charges. However, the charges are generally not transferable to very different configurations of the system since polarization effects are configuration dependent. Exceptions are cases where the conformation remains close to the optimized structure, such as in studies of rigid DNA quadruplexes and intermediate structures of the OEC of PSII shown to be very similar at very low temperatures as evidenced by X-ray absorption data (Haumann et al., 2005), the studies of enzyme catalysis with electron transfer and proton transport (Ilan, Tajkhorshid, Schulten, & Voth, 2004; Lobaugh & Voth, 1996; Okamura & Feher, 1992; Popovic & Stuchebrukhov, 2004; Sham, Muegge, & Warshel, 1998, 1999; Warshel, 1981; Warshel & Aqvist, 1991), ion channels (Aqvist & Luzhkov, 2000; Bliznyuk, Rendell, Allen, & Chung, 2001; Ilan et al., 2004; Luzhkov & Aqvist, 2000), docking and ligand binding (Cho, Guallar, Berne, & Friesner, 2005; Grater, Schwarzl, Dejaegere, Fischer, & Smith, 2005; Lappi et al., 2004; Norel, Sheinerman, Petrey, & Honig, 2001; Sheinerman & Honig, 2002; Simonson, Archontis, & Karplus, 1997, 1999; Vasilyev & Bliznyuk, 2004; Wang, Donini, Reyes, & Kollman, 2001), macromolecular assembly (Norel et al., 2001; Sheinerman, Norel, & Honig, 2000; Wang et al., 2001), and signal transduction (Gentilucci, Squassabia, & Artali, 2007; Green, Dennis, Fam, Tidor, & Jasanoff, 2006; Hurley, 2006; Mulgrew-Nesbitt et al., 2006). Therefore, the range of potential applications of MOD-QM/MM is wide and addresses the need for descriptions based on ab initio quality ESPs in biomolecular systems (Exner & Mezey, 2002, 2003, 2004, 2005; Gao et al., 2004; Kitaura et al., 2001; Li et al., 2005; Nakano et al., 2000, 2002; Szekeres, Exner & Mezey, 2005).

2.2.1 MOD-QM/MM Dangling Bonds

The interface between high and low layers often has to be drawn across covalent bonds. To address the electron density of "dangling" bonds at the QM–MM interface, a number of methods were developed (Lin & Truhlar, 2005). One of the earliest approaches is the link H-atom scheme that completes the covalency of the high layer with capping hydrogen atoms (Eurenius, Chatfield, Brooks, & Hodoscek, 1996; Field et al., 1990; Singh & Kollman, 1986). When the QM–MM interface is defined by breaking C–C bond, the hydrogen atom link is most suitable due to the similarity in

electronegativities between hydrogen and carbon atoms. However, other atoms or functional groups can be used as well (Antes & Thiel, 1999; Chen, Zhang, & Zhang, 2004; Gao et al., 2004; Zhang, Chen, & Zhang, 2003). For instance, when it is necessary to simulate electron donation or withdrawal, using halogen-like atoms—pseudohalogens—have proved useful (Zhang, Lee, & Yang, 1999). Other methods to treat the QM/MM boundary use frozen orbitals (Gao, Amara, Alhambra, & Field, 1998; Murphy, Philipp, & Friesner, 2000a; Murphy et al., 2000b; Philipp & Friesner, 1999), pseudopotentials (Bergner, Dolg, Kuchle, Stoll, & Preuss, 1993; Estrin, Tsoo, & Singer, 1991; Zhang et al., 1999), or electron density-derived schemes (Ferre & Angyan, 2002), which does not require insertion of extra atoms. In particular, the delocalized Gaussian MM method (Das et al., 2002) is implemented in the CHARMM/GAMESS-UK and CHARMM/GAMESS-US software programs (Brooks et al., 1983). A comparative study was carried out by Karplus and coworkers, who showed that link atoms and frozen orbitals method give comparable results and neither is systematically better than the other (Reuter, Dejaegere, Maigret, & Karplus, 2000). In practice, the Gaussian ONIOM implementations of MOD-QM/MM use hydrogen link atoms (Dapprich et al., 1999; Humbel et al., 1996; Maseras & Morokuma, 1995; Svensson et al., 1996; Vreven et al., 2001; Vreven & Morokuma, 2000a, 2003), while calculations based on the Qsite package (Murphy et al., 2000a, 2000b; Philipp & Friesner, 1999) use frozen orbitals. However, MOD-QM/MM in general is not limited to any particular treatment of dangling bonds. While neither Gaussian nor Qsite software packages have not yet implemented the MOD-QM/MM method as a built-in algorithm that could be invoked with a keyword, the software can be run as a free standalone software package in conjunction with Gaussian or Qsite, as described in the user guide posted at http://gascon.chem.uconn.edu/software.

2.2.2 MOD-QM/MM ESP Charges

The ESP atomic charges of individual molecular fragments obtained by the MOD-QM/MM method (Gascon, Leung, et al., 2006) are computed according to a least-squares fit procedure similar to the Besler–Merz–Kollman method, implemented in Gaussian (Besler, Merz, & Kollman, 1990). In the least squares fit procedure, the following function is minimized:

$$\gamma(q_1, q_2, \ldots, q_N) = \sum_{j=1}^{m} \left(V_j - E_j\right)^2 + \sum_k \lambda_k g_k(q_1, q_2, \ldots, q_N), \qquad (2)$$

where V_j is the ab initio ESP at a space point j and $E_j = \sum_{k=1}^{N} q_k / r_{jk}$ and λ_k represents the Lagrange multiplier imposing the constraint. In the Besler–Merz–Kollman method, a single constraint is used, which ensures that the sum of the atomic charges equals the total charge of the fragment: $g_1(q_1, q_2, \ldots, q_N) = \sum_{K=1}^{N} q_k - q_{tot} = 0$, where N is the number of atoms in the QM layer. In MOD-QM/MM approach, such a scheme would lead to charge leakage to the capping fragments and, therefore, would change the total charge of the system along subsequent iterations. Therefore, the MOD-QM/MM method introduces another constraint to ensure that the sum of the charges of link atoms is equal to zero: $g_1(q_1, q_2, \ldots, q_N) = \sum_{K=1}^{N-M} q_k = 0$, where $N-M$ is the number of link atoms (Fig. 3).

In the MOD-QM/MM method, the ESP charges are obtained by considering a QM layer with N atoms, including atoms whose charges would be fitted (region 1), atoms whose charges are not fitted (region 2), and $N-M$ link H-atoms. Often, nearest neighbor residues are included as capping

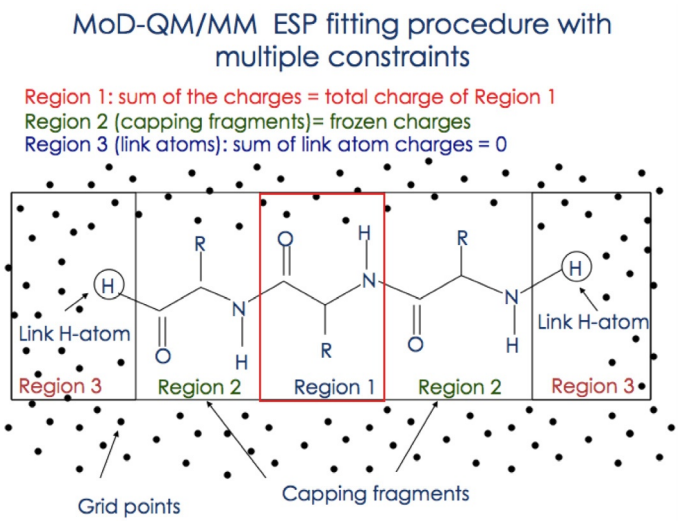

Fig. 3 Charge constraints for fitting the electrostatic potential of a domain (region 1) according to the MOD-QM/MM method (Gascon, Leung, et al., 2006), when capped by nearest neighbor residues (region 2) and link hydrogen atoms.

fragments (region 2) to separate the domain whose charges would be fitted (region 1) from the QM/MM interface (Fig. 3) and avoid over-polarization effects. The total charge of the QM layer is $Q = Q_1 + Q_2$, where $Q_1 = \sum_{i=1}^{M-1} q_i + q_M$ is the net charge of the fragment and $Q_2 = \sum_{i=M+1}^{N-1} q_i + q_N$ is set equal to zero. The ESP at position r_j, due to all point charges in the QM region, is $u_j = \sum_{i=1}^{N} q_i / r_{ji}$ where $r_{ji} = |r_j - r_i|$.

Considering the conditions imposed for Q_1 and Q_2 the ESP becomes,

$$u_j = \sum_{i=1}^{M-1} \left[\frac{q_i}{r_{ji}} - \frac{q_i}{r_{jM}} \right] + \frac{Q_1}{r_{jM}} + \sum_{i=M+1}^{N-1} \left[\frac{q_i}{r_{ji}} - \frac{q_i}{r_{jN}} \right] + \frac{Q_2}{r_{jN}}. \tag{3}$$

Substituting $F_{jik} = \left(1/r_{ji} - 1/r_{jk}\right)$ and $K_{jk} = 1/r_{jk}$, Eq. (3) can be rewritten as follows:

$$u_j = \sum_{i=1}^{M-1} q_i F_{jiM} + \sum_{i=M+1}^{N-1} q_i F_{jiN} + Q_1 K_{jM} + Q_2 K_{jN}. \tag{4}$$

To compute the ESP atomic charges, a least-square minimization procedure of the error function $\chi^2 = \sum_{j=1}^{N_g} \left(u_j - U_j\right)^2$ is performed, where U_j is the QM/MM ESP at grid point j and u_j is the corresponding ESP as defined by the distribution of point charges. The sum is typically carried over the set of N_g grid points, associated with four layers at 1.4, 1.6, 1.8, and 2.0 times the van der Waals radii around the QM region span the N_g grid points (Fig. 3). The minimum of χ^2 is obtained by the following gradient:

$$\frac{\partial \chi^2}{\partial q_k} = -\sum_{j=1}^{N_g} 2\left(u_j - U_j\right) \frac{\partial u_j}{\partial q_k} = 0, \tag{5}$$

for all q_k in the set $(q_1, q_2, \ldots, q_{M-1}, q_{M+1}, \ldots, q_{N-1})$. Since $\frac{\partial u_j}{\partial q_k} = F_{jks}$, where s corresponds to M or N depending on whether $k < M$ or $M < k < N$, respectively, we can rewrite Eq. (5):

$$\sum_{j=1}^{N_g}\left[U_j-\left(Q_1K_{jM}+Q_2K_{jN}\right)\right]F_{jks}=\sum_{i=1}^{M-1}q_i\sum_{j=1}^{N_g}F_{jiM}F_{jks}-\sum_{i=M+1}^{N-1}q_i\sum_{j=1}^{N_g}F_{jiN}F_{jks}. \tag{6}$$

Or, in matrix notation:

$$c=q\begin{bmatrix}F_1 & 0\\ 0 & F_2\end{bmatrix}, \tag{7}$$

where

$$c^k=\sum_{j=1}^{N_g}\left[U_j-\left(Q_1K_{jM}+Q_2K_{jN}\right)\right]F_{jks},$$
$$q=(q_1,q_2,\ldots,q_{M-1},q_{M+1},\ldots,q_{N-1}),$$

$F_1^{lk}=\sum_{j=1}^{N_g}F_{jlM}F_{jks}$, and $F_2^{lk}=\sum_{j=1}^{N_g}F_{jlN}F_{jks}$. Note that vector c and matrix F are only functions of distances between atomic positions. The grid points r_{jk}, the partial charges Q_1 and Q_2, and the ESP are evaluated at grid points $j=1,\ldots,N_g$.

2.2.3 MOD-QM/MM Optimization

In MOD-QM/MM, the total system is divided into molecular domains and an iterative cycle of QM/MM calculations is performed. In each step, a different molecular domain is considered as a QM layer, for which a geometry relaxation is performed and the ESP atomic charges are updated. The rest of the system is treated at the MM level with atomic charges defined as updated along the MOD-QM/MM iterations. The iterative scheme was initially developed for ab initio computations of protein ESPs (Gascon, Leung, et al., 2006) and was recently generalized for self-consistent structural refinement of extended systems (Ho et al., 2014).

Geometry optimization is typically carried out using the Newton–Raphson method (Fan & Ziegler, 1991; Versluis & Ziegler, 1988), and the Hessian matrix is updated with the Broyden–Fletcher–Goldfarb–Shanno strategy (Schlegel, 1987). Initially, the geometry of the first domain (R_1) is optimized taking into account the surrounding environment. In its minimum energy configuration, the ESP charges of the QM layer are computed and used to update the charges of that domain when treated at the MM level in subsequent steps of the iterative cycle. The procedure is applied analogously to all domains, and the cycle is iterated multiple times until the

geometry and distribution of atomic charges converge self-consistently as influenced by mutual polarization effects. Recently, the approach was applied to characterize the hydrogen-bonded geometry of the DNA *Oxytricha nova* guanine quadruplex (G4), showing results comparable to the full QM calculations (Ho et al., 2014).

ONIOM-EE Optimization: Interactions between QM and MM layers in MOD-QM/MM are often dominated by the electrostatic terms. In the ONIOM electronic embedding (EE) scheme (Vreven et al., 2006; Vreven & Morokuma, 2000b; Vreven, Morokuma, Farkas, Schlegel, & Frisch, 2003), the electrostatic interactions are included as one-electron operators of the QM Hamiltonian. The atom-centered partial point charges in the QM Hamiltonian give rise to the ESP due to the MM layer. Other types of interactions between QM and MM layers, such as bonding and non-bonding Van der Waals terms, are also retained at the MM level.

Optimization according to the ONIOM implementation of MOD-QM/MM is performed by following the total energy gradient:

$$\frac{\partial E^{ONIOM}}{\partial q} = \frac{\partial E_X^{QM}}{\partial q} \cdot \mathbf{J} + \frac{\partial E_{X+Y}^{MM}}{\partial q} - \frac{\partial E_X^{MM}}{\partial q} \cdot \mathbf{J} \tag{8}$$

where $\mathbf{J}$ is the Jacobian necessary to transform the coordinates of the reduced system (X) into the coordinates of the complete system ($X+Y$). Initially, the coordinates of the reduced system are frozen, leaving only the second term of the expansion. This leads to optimization of the full system at MM level through microiterations. Then, a QM energy minimization step is performed to update the coordinates of the reduced system, based on the forces calculated according with Eq. (8). Microiterations are repeated until the total energy converges to a minimum with respect to all nuclear coordinates.

In the ONIOM electronic embedding (EE) method, $\partial E_X^{QM}/\partial \mathbf{q}^Y \neq 0$ and $\partial E_X^{MM}/\partial \mathbf{q}^Y \neq 0$, that is why the coordinates of the system cannot be rigorously separated into $\mathbf{q}^X$ and $\mathbf{q}^Y$, making the abovementioned microiteration scheme not applicable. In the ONIOM implementation, this issue is addressed by approximating the electrostatic interactions between QM and MM layers during the microiterations, as described by the distribution of ESP charges computed for the initial configuration. After the microiterations are completed, with essentially a frozen distribution of atomic charges, the wave function of the QM layer is reevaluated giving rise to new ESP charges for subsequent microiterations. The QM wave function is recomputed and the MM geometry is reoptimized several times until a self-consistent solution is

obtained. Only after that, the QM energy minimization step is performed, and the coordinates of the QM layer are updated. This double self-consistency process is repeated until convergence is reached.

2.2.4 MOD-QM/M Model of the OEC of Photosystem II

MOD-QM/MM models of the OEC of PSII have been originally based on the 1S5L X-ray crystal structure of cyanobacterium PSII (Ferreira, Iverson, Maghlaoui, Barber, & Iwata, 2004) and more recently refined in light of recent breakthroughs in conventional and femtosecond X-ray crystallography (Askerka, Vinyard, Wang, Brudvig, & Batista, 2015; Askerka, Wang, Brudvig, & Batista, 2014; Li, Siegbahn, & Ryde, 2015; Luber et al., 2011; Pal et al., 2013). The models included the Mn_3CaO_4Mn OEC cluster and all amino acid residues with α-carbons within 15 Å from any atom in the OEC, resulting in a total of 1987 atoms. Water ligands were added to complete the coordination spheres of the Mn and Ca atoms, while keeping the displacement of the amino acid residues at minimum. This led to the characteristic coordination numbers of 5 or 6, 6 for Mn^{III}, Mn^{IV} and 8 for Ca, respectively. The presence of at least one water molecule bound to Ca^{2+} is suggested by ^{18}O isotope exchange measurements (Hillier & Wydrzynski, 2004, 2008). The resulting structure of the OEC hydration shell is consistent with pulsed EPR experiments, revealing the presence of several exchangeable deuterons near the Mn cluster in the S_0, S_1, and S_2 states (Britt et al., 2004).

MOD-QM/MM computations of the OEC of PSII required high-quality initial guesses of the QM layer electronic structure, including a proper description of spin states in the OEC cluster as directly compared to spectroscopic measurements. These were originally obtained by using the ligand field theory as implemented in Jaguar 5.5 (Schrodinger, 2003, Jaguar, Portland, OR) and most recently according to the spin fragment approach as implemented in Gaussian 09. Once the initial state was properly defined, it was used within the ONIOM approach as the QM layer of MOD-QM/MM calculations (region X), including the Mn_3CaO_4Mn OEC complex, water molecules, hydroxide and chloride ions in the OEC vicinity, as well as the directly ligated carboxylate groups of D1-D189, CP43-E354, D1-A344, D1-E333, D1-D170, D1-D342, and the imidazole ring of D1-H332 amino acid residues (Fig. 4). The QM/MM interface was defined by breaking C–C bonds of side chains in the abovementioned amino acid residues. Capping of the QM layer was based on the link hydrogen atom scheme. The molecular structure beyond the

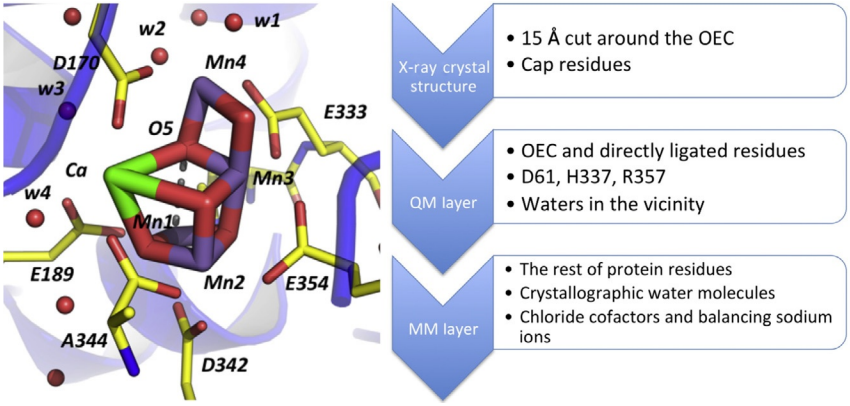

Fig. 4 *Left*: Structural model of the OEC of PSII (QM layer shown explicitly, MM layer shown as cartoon). *Right*: Scheme of QM/MM model preparation.

QM layer was treated using Amber classical force field (Cornell et al., 1995). A protein buffer shell with amino acid residues with α-carbons within 15–20 Å from any atom in the OEC ion cluster was also added with harmonic constraints to preserve the natural shape of the system even in the absence of the rest of the protein complex and membrane.

An important aspect of the OEC cluster is the antiferromagnetic coupling between manganese centers. These were simulated using broken-symmetry states (Noodleman, 1981; Noodleman & Case, 1992; Noodleman & Davidson, 1986; Noodleman, Peng, Case, & Mouesca, 1995) in conjunction with DFT. The QM layer was prepared in various spin states and the spin coupling patterns were stabilized by ligand arrangement. Upon optimization, the resulting structures are analyzed in terms of the total energy as well as by comparison of structural and electronic features to experimental data from high-resolution spectroscopy (EPR).

2.2.5 Post-QM/MM Structural Refinement Based on Spectroscopic Data

Typically, potential energy surfaces (PESs) of biological systems are very rugged, with many local minima of comparable in energy. It is, therefore, often difficult to find a subset of configurations with maximum statistical weight by energy minimization. However, it is possible to implement a post-QM/MM structural refinement scheme that addresses the likelihood of energetically similar structures in terms of their consistency with the high-resolution spectroscopy (for instance, EXAFS) (Pal et al., 2013; Sproviero, Gascon, et al., 2008c).

The refinement algorithm starts with a reference configuration of the system (eg, the QM/MM minimum energy structure) and iteratively adjusts the nuclear coordinates to minimize the mean square deviation between the simulated and experimental spectra by simulated annealing Monte Carlo (MC). Each MC step consists of an attempt to move all atoms of choice according to the Metropolis algorithm. The probability of accepting the new position is given by: $P = \min[1, e^{-\Delta F/kT}]$, where k is the Boltzmann constant, T is the temperature (which in this case is varied exponentially from an initial value to 0 K), and ΔF denotes the difference in the cost function, defined as the sum of squared differences between experimental and calculated spectra, when comparing the displaced and undisplaced configurations (Fig. 5). In previous applications, the cost function has been calculated by taking the sum of the square deviations between the experimental and calculated EXAFS spectra. Normally, the simulation is performed by harmonically constraining all the surrounding ligands and relaxing the metal oxide core of the OEC, restricting the displacements to those of the atoms in the OEC and surrounding ligands known to be responsible for affecting the

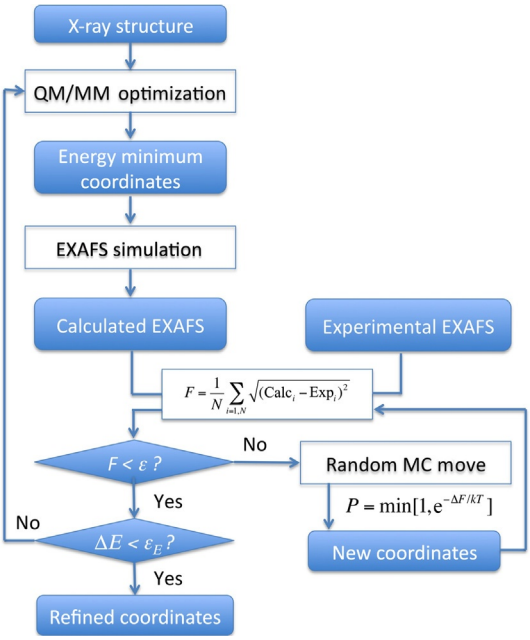

Fig. 5 Post-QM/MM structural refinement scheme based on EXAFS calculations and simulated annealing MC (Pal et al., 2013).

experimental EXAFS of S-state intermediates. To harmonically constrain the atoms, an additional penalty of $k^*||r - r_{\text{int}}||^2$ is added to the cost function, where $r - r_{\text{int}}$ is the displacement vector with respect to the initial position r_{int}. The EXAFS spectra for a given configuration of the system are computed by calls to the external program FEFF8 (version 8.2) (Ankudinov, Bouldin, Rehr, Sims, & Hung, 2002a; Ankudinov, Ravel, Rehr, & Conradson, 1998; Bouldin, Sims, Hung, Rehr, & Ankudinov, 2001).

It is important to note that even though the post-QM/MM structural refinement algorithm has been implemented for EXAFS spectra simulations, the ΔF minimization procedure could also be based on other spectroscopic data whenever experimental data are available and the calculated spectra can be reliably and efficiently computed. Examples include calculations of EPR data or NMR chemical shifts.

3. EXAFS SIMULATIONS

Ab initio simulations of EXAFS spectra involve solving the multi-scattering problem associated with the photodetached electrons emitted upon X-ray absorption by the Mn centers. The quantum mechanical interference of outgoing photoelectrons with the backscattering waves from atoms surrounding the Mn ions gives rise to oscillations of X-ray absorption intensities as a function of the kinetic energy (or momentum) of the photodetached electron. The Fourier transform of these oscillations provides information on the Mn–Mn distances, the coordination of Mn ions, and changes in the Mn coordination sphere as determined by changes in the oxidation state of the metal centers. Calculations are typically carried out according to the real-space Green function approach, as implemented in the program FEFF8 (version 8.2) (Ankudinov et al., 2002a, 1998; Bouldin et al., 2001), using the theory of the oscillatory structure due to multiple scattering originally proposed by Kronig (Kronig, 1931; Kronig & Penney, 1931) and worked out in detail by Sayers (Sayers, Stern, & Lytle, 1971), Stern (Stern, 1974), Lee and Pendry (Lee & Pendry, 1975), and by Ashley and Doniach (Ashley & Doniach, 1975). In FEFF, the EXAFS spectrum is calculated according to the following equation:

$$\chi(k) = \sum_j \frac{N_j f_j(k) e^{-2k^2\sigma_j^2}}{kR_j^2} \sin\left[2kR_j + \delta_j(k)\right], \tag{9}$$

where $f(k)$ and $\delta(k)$ are scattering properties (amplitudes and phase shifts) of the atoms neighboring the excited atom, N is the number of neighboring atoms, R is the distance to the neighboring atom, and σ^2 is a measure of the disorder in the neighbor distance.

EXAFS using Mn atoms as absorption centers has been particularly important in structural characterization of the OEC in PSII (Dau, Grundmeier, Loja, & Haumann, 2008; Dau & Haumann, 2008; Haumann et al., 2005; Yano et al., 2006). Unlike X-ray diffraction experiments, the X-ray intensities used for EXAFS do not induce radiation damage (Davis & Pushkar, in press; Galstyan, Robertazzi, & Knapp, 2012; Luber et al., 2011; Pal et al., 2013; Pantazis, Ames, Cox, Lubitz, & Neese, 2012) to highly charged (III–IV) Mn (Yano et al., 2005). The onset of radiation damage can be precisely determined and controlled by monitoring the absorber metal K-edge position, allowing us to use as a reference an (almost) intact metal cluster within the protein. In addition, EXAFS provides metal-to-metal and metal-to-ligand distances with high accuracy (~0.02 Å) and a resolution of ~0.1 Å (Askerka et al., 2015) and can be performed in solution allowing for capturing the intermediate (S_n states) in the PSII catalytic cycle (Haumann et al., 2005). The latter analysis in combination with highly accurate computational tools to predict the EXAFS spectrum (Ankudinov, Bouldin, Rehr, Sims, & Hung, 2002b; Newville, 2001) has been extensively exploited by the computational groups as it allows for direct comparisons to DFT and hybrid QM/MM models of the PSII intermediates with the experimental spectroscopic data (Askerka et al., 2015, 2014; Li et al., 2015; Luber et al., 2011; Pal et al., 2013).

3.1 Post-QM/MM Refinement Model of the OEC of PSII

Structural refinement proved to be particularly useful when dealing with subtle changes in structure that may affect the EXAFS spectrum, such as those produced by changes in protonation states of the μ-oxo bridges in the PSII OEC. For example, in Pal et al. (2013), it was important to determine the protonation states of the O4 and O5 μ-oxo bridges in the S_0 state of PSII. It is known that S_0 to S_1 transition in the catalytic cycle includes release of the proton; however, its position in S_0 state remained known. To understand the nature of deprotonation proton, a preliminary MC screening was conducted using simulated annealing to fit the S_0 EXAFS data, as based on the geometry of the previously reported S_1 model. The model was composed of the metal oxide cluster, the functional groups of the residues which are directly coordinated, and the hydrogen-bonded water network around

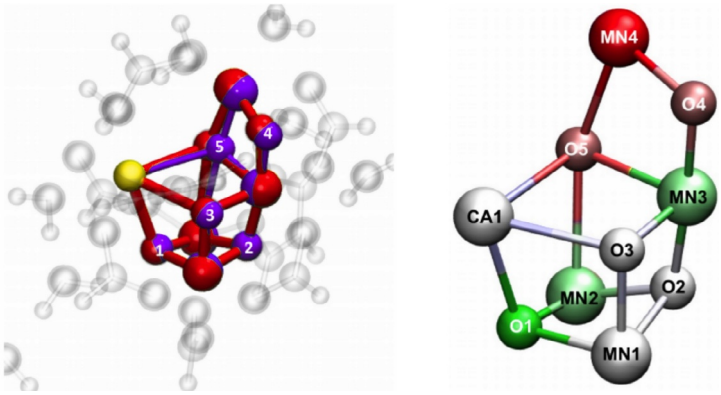

Fig. 6 Monte Carlo (MC)-refined OEC cluster of the S_0 state (in *red* (*gray* in the print version)) and S_1 state (in *purple* (*dark gray* in the print version)) structures (*left*) and the crystal structure B-factors for the atoms in the OEC with most certain positions colored *green* (*light gray* in the print version) and least certain (Mn4 and corresponding bridges) colored *red* (*gray* in the print version) (*right*) (Pal et al., 2013). *Pal, R., Negre, C.F.A., Vogt, L., Pokhrel, R., Ertem, M.Z., Brudvig, G.W., & Batista, V.S. (2013). S_0-state model of the oxygen-evolving complex of photosystem II,* Biochemistry, *52(44), 7703–7706. http://dx.doi.org/10.1021/bi401214v. Copyright American Chemical Society 2013.*

the OEC. An overlay of the OEC geometry for the MC-prescreened S_0 state and the S_1 state is shown in Fig. 6.

MC refinement showed that the main difference in the S_0 EXAFS when compared to S_1 is in positions of Mn3, Mn4, O4, and O5 atoms. These results suggested that the proton may originate from the O5 or O4 μ-oxo bridge in the S_0 state. Since the S_0 to S_1 transition also involves an electron release, the movement of Mn3 and Mn4 in the MC refinement indicated that one of those Mn centers may be responsible for oxidation. Interestingly, this is in agreement with the reported B-factors of the atoms in X-ray crystal structure at 1.9 Å resolution (PDB: 3ARC) (Umena, Kawakami, Shen, & Kamiya, 2011). The O4 and O5 atoms exhibit the highest displacement among all the bridging μ-oxos (see Fig. 6, left), which could originate from radiation damage and partial reduction of the resting S_1 state to S_0. Therefore, the next step was to explore the protonation of O4 and O5 sites using the QM/MM model of the S_0 state:

Fig. 7 shows that the 8–11.6 $Å^{-1}$ region of the experimental EXAFS is more consistent with O5 protonated compared to O4 protonated. While both of the refined QM/MM models for both O5-H and O4-H fit well, RMSD of the $CaMn_4O_5$ cluster for O5-H is much lower (0.05 Å) than the RMSD for O4-H (0.12 Å), indicating that smaller refinements are needed

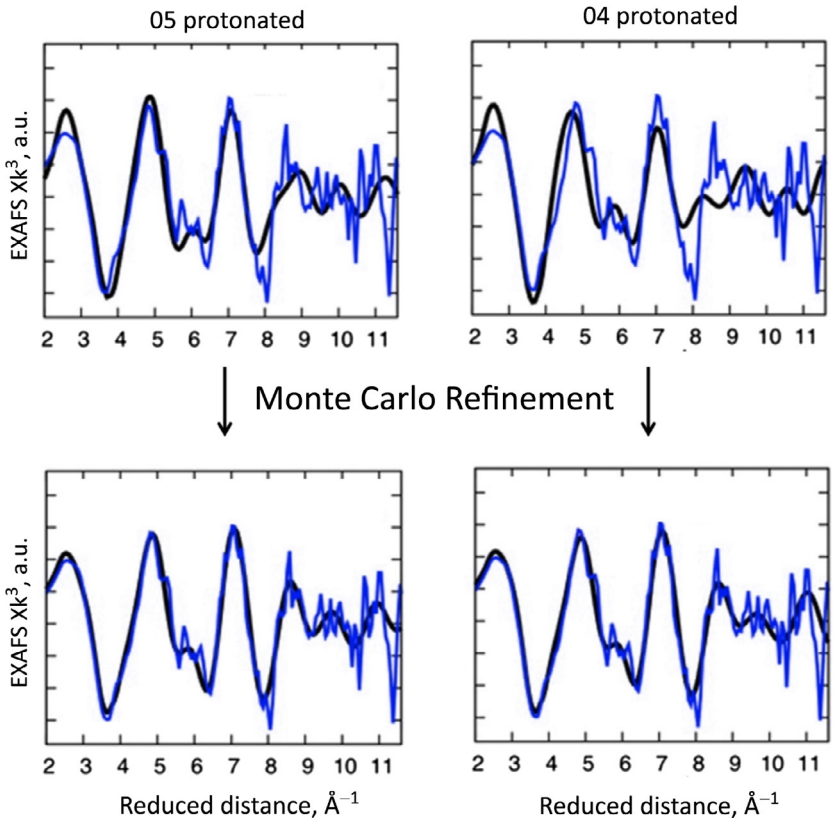

Fig. 7 EXAFS spectra of the S_0 state of the OEC with O5 (*left*) and O4 (*right*) protonated as well as corresponding MC refined spectra (*bottom*) (Pal et al., 2013). *Pal, R., Negre, C.F.A., Vogt, L., Pokhrel, R., Ertem, M.Z., Brudvig, G.W., & Batista, V.S. (2013). S_0-state model of the oxygen-evolving complex of photosystem II,* Biochemistry, 52*(44), 7703–7706. http://dx.doi.org/10.1021/bi401214v*.

to get a good match to experimental EXAFS. Upon inspection, we find that the O5-H structure shows minimal movements, whereas O4-H undergoes more significant structural changes during the MC refinement. This serves as another proof that QM/MM O5-H structure is most likely representative of the actual S_0 state observed by EXAFS measurements.

4. MOD-QM/MM MODELS OF DNA QUADRUPLEXES

MOD-QM/MM applications have produced various structural models that could be partially validated by direct comparisons with experimental

data, including NMR, EXAFS, X-ray diffraction, and calorimetry measurements (Gascon, Leung, et al., 2006; Gascon et al., 2008; Menikarachchi & Gascon, 2008; Sproviero et al., 2006a; Sproviero, Gascon, McEvoy, Brudvig, & Batista, 2006b; Sproviero et al., 2007; Sproviero, Gascon, et al., 2008a, 2008b, 2008c, 2008d; Sproviero, Gascon, et al., 2008b). Recently, a benchmark MOD-QM/MM study has focused on the DNA *Oxytricha nova* guanine quadruplex (Ho et al., 2014), including direct comparisons to high-resolution X-ray diffraction (Haider, Parkinson, & Neidle, 2002, 2003) and NMR data (Gill, Strobel, & Loria, 2006). The DNA quadruplex has a central channel containing five potassium ions (K^+ shown in yellow in Fig. 8) in between layers of guanine quartets (shown in orange in Fig. 8) that are essential for stabilizing the quadruplex structure. The presence of these ions introduces significant polarization effects that are not adequately described by static molecular mechanics force fields. This is manifested by a very loosely bound potassium ion in the thymine loops (shown in gray in Fig. 8) of the quadruplex, as well as convergence to the incorrect bifurcated hydrogen bonding geometry of the guanine quartets (Gkionis et al., 2014; Song, Ji, & Zhang, 2013).

For comparison, Fig. 9 shows a rigid scan of the PES for a two-layer model where a potassium ion is displaced stepwise along the z-direction. The comparison of PES profiles shows significant deviations between results

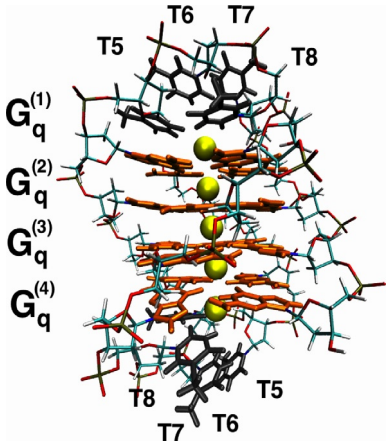

Fig. 8 1JPQ crystal structure of the DNA *Oxytricha nova* guanine quadruplex. *Ho, J., Newcomer, M.B., Ragain, C.M., Gascon, J.A., Batista, E.R., Loria, J.P., & Batista, V.S. (2014). MoD-QM/MM structural refinement method: Characterization of hydrogen bonding in the Oxytricha nova G-Quadruplex,* Journal of Chemical Theory and Computation, 10*(11), 5125–5135. http://pubs.acs.org/doi/full/10.1021/ct500571k. Copyright American Chemical Society 2014.*

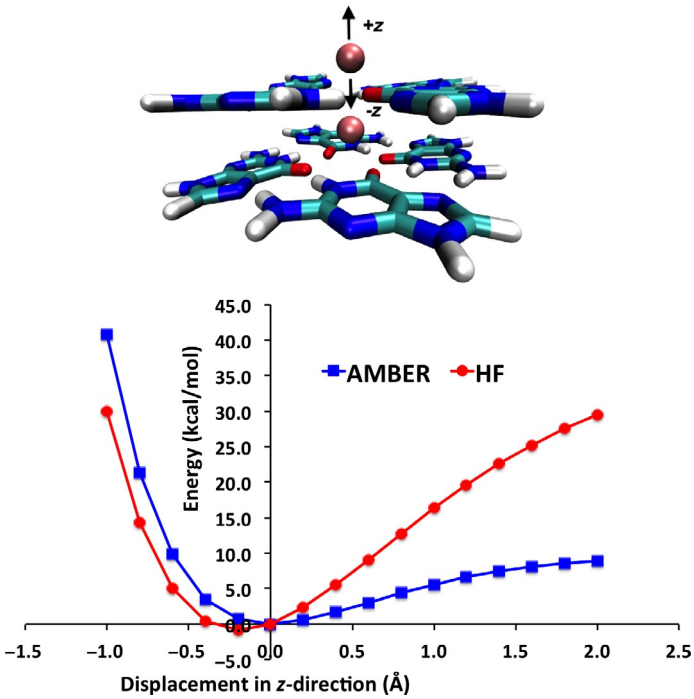

Fig. 9 Benchmark calculations of electrostatic interactions for a potassium ion dragged through the internal channel of a two-layer model of the DNA guanine quadruplex, as described by HF and Amber, revealing significant polarization effects missed by non-polarizable molecular mechanics force fields.

obtained with HF and the Amber molecular mechanics force field. In particular, the force field substantially underestimates the binding energy of the potassium ion because it does not account explicitly for mutual polarization effects. Therefore, electrostatic stabilization of the monovalent cations by the guanine quartets is underestimated.

The main goal of the MOD-QM/MM study has been to explore the refinement of the G-quadruplex geometry that is sensitive to electrostatic interactions between the embedded K^+ ions and the polarized guanine moieties, and to validate the resulting MOD-QM/MM models through direct comparison of ^{1}H NMR chemical shifts (Ho et al., 2014) which are very sensitive to the detailed configuration of hydrogen bonding in the folded quadruplex configuration. Therefore, it was important to describe electrostatic interactions and polarization effects accurately since K^+ ions polarize the guanine moieties and affect the hydrogen bonds and stacking interactions that regulate the NMR chemical shifts. As shown in Fig. 10, the

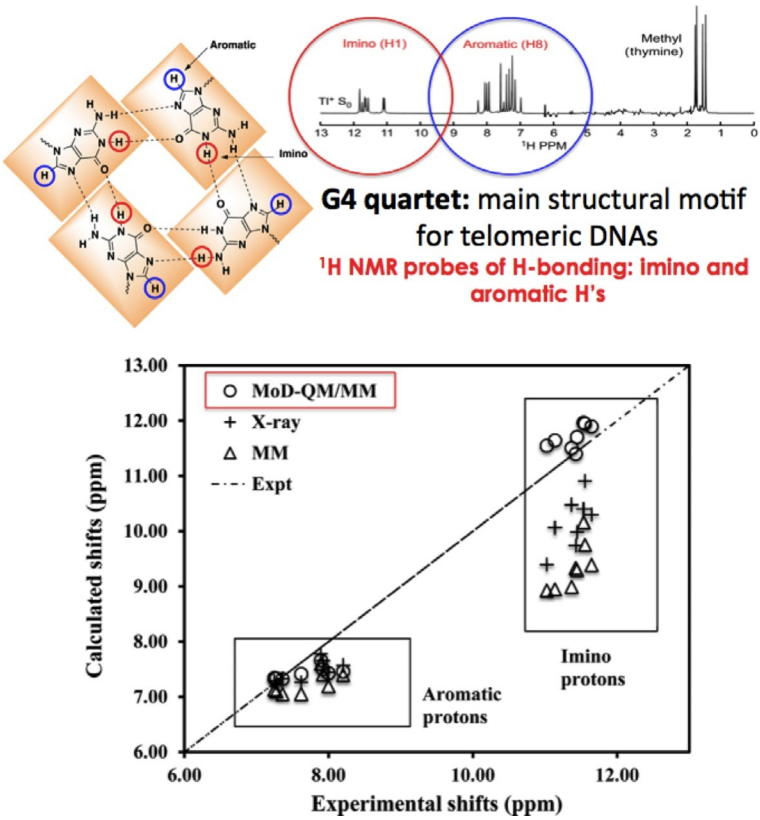

Fig. 10 Comparison of experimental and calculated ^{1}H NMR chemical shifts, obtained at the ONIOM(ωB97XD/6-31G(d,p):AMBER)-EE level of theory for MOD-QM/MM structural models (*circles*), and structures predicted by a classical molecular mechanics (AMBER) force field (*triangles*) and the X-ray structure (*crosses*). *Copyright American Chemical Society 2014.*

MOD-QM/MM refined structure gives a significant improvement in the description of the chemical shifts when compared to those predicted by popular molecular mechanics force fields (Ho et al., 2014).

The MOD-QM/MM model of the DNA quadruplex (Haider et al., 2002) was prepared from the 1JPQ X-ray crystal model by using the standard protocol of adding hydrogen atoms and solvating the resulting structure in a periodic box of water molecules. Classical molecular dynamics simulations equilibrated the solvated system while constraining the quadruplex structure. Production run calculations were based on an ensemble of solvated configurations, composed of the quadruplex and water molecules within 15 Å from any atom in the G4 quadruplex. For each representative

configuration of the quadruplex, molecular domains were defined as individual guanine nucleotides within quartets. Accordingly, the hydrogen bonding interactions between the nucleotides were described at the MM level, albeit using MOD-QM/MM-restrained ESP charges. Then, the MOD-QM/MM iterative algorithm was implemented where each of the 16 nucleotides is treated as the QM layer in an ONIOM (ωB97XD/6-31G(d):Amber) calculation while keeping fixed all other domains. The geometry of the QM layer was relaxed in the presence of the surrounding charges, and the restrained ESP charges were calculated on the converged geometry. The cycle then proceeded to the next domain, using the atomic charges and geometry updated from the previous QM/MM calculation, and the cycle was complete when the algorithm iterated over all 16 domains and was iterated until the charges and geometry of each domain were converged below a desired threshold tolerance value.

Proton NMR chemical shifts were then calculated using the gauge-independent atomic orbital (GIAO) method at the DFT QM/MM (ωB97XD/6-31G(d):Amber) level for each of the solvated configurations after structural refinement based on the MOD-QM/MM method. To account for the shielding effects between the guanine quartets, the QM layer included all 16 nucleotides. The NMR chemical shifts were then obtained as an average over solvated configurations, sampled from classical MD simulations. The overall average yielded proton NMR chemical shifts for the imino- and aromatic protons that are within 0.5 ppm from experimental data.

5. CONCLUSIONS

Establishing a simple and reliable approach to describe electrostatic interactions in complex molecular systems, including the influence of polarization effects on structural models and mechanisms, has been a long-standing challenge in computational enzymology. In this chapter, we have shown that the recently developed MOD-QM/MM hybrid method provides a rigorous yet practical approach to obtain ab initio quality models based on a simple space domain decomposition scheme and the iterative self-consistent treatment of the constituent molecular fragments, according to state-of-the-art QM/MM methods.

The MOD-QM/MM method has been successfully applied to complex biological systems, including important applications to PSII, human aldose reductase enzyme, and guanine DNA quadruplexes, demonstrating the capabilities of the method as applied to systems where electrostatic

interactions are critical. The post-QM/MM refinement methodology allows to assess structures of similar energy and to explore subtle structural changes, including those induced by monovalent cations or variable protonation states, as directly compared to high-resolution spectroscopic data. The method has been developed and implemented using EXAFS computations and simulated annealing MC minimization, where the nuclear coordinates of the model are refined for best agreement between calculated and experimental spectra. While implemented in conjunction with calculations of EXAFS spectra, the methodology could be implemented more generally with other types of spectroscopic techniques (eg, FTIR, NMR) whenever experimental data are available and the calculated spectra can be reliably and efficiently computed.

We have shown that the MOD-QM/MM approach can be applied to address fundamental questions on the role of electrostatic interactions on structural refinement of PSII and DNA quadruplexes that for many years remained largely elusive to rigorous first-principles examinations. We found that the resulting QM/MM methodology, where polarization effects are explicitly considered, is a powerful tool when applied in conjunction with high-resolution spectroscopy. Therefore, it is natural to anticipate that the MPD-QM/MM approach will continue to make important contributions on enzymology-based structural and mechanistic characterization.

ACKNOWLEDGMENTS

V.S.B. acknowledges an allocation of DOE high-performance computing time from NERSC and the support from the NSF CHE-1465108 grant. Development of the MOD-QM/MM approach was partially funded by the NIH grant 1R01GM10621-01A1. We also thank Dr. Christian Negre for contributions to EXAFS-refinement methodology and Dr. Leslie Vogt for contribution to the PSII model preparation.

REFERENCES

Ankudinov, A. L., Bouldin, C. E., Rehr, J. J., Sims, J., & Hung, H. (2002a). Parallel calculation of electron multiple scattering using Lanczos algorithms. *Physical Review B: Condensed Matter*, *65*(10), 104107.

Ankudinov, A. L., Bouldin, C. E., Rehr, J. J., Sims, J., & Hung, H. (2002b). Parallel calculation of electron multiple scattering using Lanczos algorithms. *Physical Review B*, *65*(10), 104107. http://dx.doi.org/10.1103/Physrevb.65.104107.

Ankudinov, A. L., Ravel, B., Rehr, J. J., & Conradson, S. D. (1998). Real-space multiple-scattering calculation and interpretation of x-ray-absorption near-edge structure. *Physical Review B: Condensed Matter*, *58*(12), 7565–7576.

Antes, I., & Thiel, W. (1999). Adjusted connection atoms for combined quantum mechanical and molecular mechanical methods. *Journal of Physical Chemistry A*, *103*(46), 9290–9295.

Aqvist, J., & Luzhkov, V. (2000). Ion permeation mechanism of the potassium channel. *Nature (London)*, *404*(6780), 881–884.

Ashley, C. A., & Doniach, S. (1975). Theory of extended X-ray absorption-edge fine-structure (EXAFS) in crystalline solids. *Physical Review B: Condensed Matter*, *11*(4), 1279–1288.

Askerka, M., Vinyard, D. J., Wang, J. M., Brudvig, G. W., & Batista, V. S. (2015). Analysis of the radiation-damage-free X-ray structure of photosystem II in light of EXAFS and QM/MM data. *Biochemistry*, *54*(9), 1713–1716. http://dx.doi.org/10.1021/acs.biochem.5b00089.

Askerka, M., Wang, J., Brudvig, G. W., & Batista, V. S. (2014). Structural changes in the oxygen-evolving complex of photosystem II induced by the S1 to S2 transition: A combined XRD and QM/MM study. *Biochemistry*, *53*(44), 6860–6862. http://dx.doi.org/10.1021/bi5011915.

Babu, K., & Gadre, S. R. (2003). Ab initio quality one-electron properties of large molecules: Development and testing of molecular tailoring approach. *Journal of Computational Chemistry*, *24*(4), 484–495.

Babu, K., Ganesh, V., Gadre, S. R., & Ghermani, N. E. (2004). Tailoring approach for exploring electron densities and electrostatic potentials of molecular crystals. *Theoretical Chemistry Accounts*, *111*(2–6), 255–263.

Bader, J. S., & Berne, B. J. (1996). Solvation energies and electronic spectra in polar, polarizable media: Simulation tests of dielectric continuum theory. *Journal of Chemical Physics*, *104*(4), 1293–1308.

Bakowies, D., & Thiel, W. (1996). Hybrid models for combined quantum mechanical and molecular mechanical approaches. *Journal of Physical Chemistry*, *100*(25), 10580–10594.

Baldwin, M. J., Kampf, J. W., & Pecoraro, V. L. (1993). The linear MnII complex $Mn_3(5\text{-}NO_2\text{-}Salimh)_2(Oac)_4$ provides an alternative structure type for the carboxylate shift in proteins. *Journal of the Chemical Society, Chemical Communications*, (23), 1741–1743.

Banks, J. L., Kaminski, G. A., Zhou, R. H., Mainz, D. T., Berne, B. J., & Friesner, R. A. (1999). Parametrizing a polarizable force field from ab initio data. I. The fluctuating point charge model. *Journal of Chemical Physics*, *110*(2), 741–754.

Bergner, A., Dolg, M., Kuchle, W., Stoll, H., & Preuss, H. (1993). Ab-Initio energy-adjusted pseudopotentials for elements of groups 13-17. *Molecular Physics*, *80*(6), 1431–1441.

Bernardo, D. N., Ding, Y. B., Kroghjespersen, K., & Levy, R. M. (1994). An anisotropic polarizable water model—Incorporation of all-atom polarizabilities into molecular mechanics force-fields. *Journal of Physical Chemistry*, *98*(15), 4180–4187.

Besler, B. H., Merz, K. M., & Kollman, P. A. (1990). Atomic charges derived from semi-empirical methods. *Journal of Computational Chemistry*, *11*(4), 431–439.

Bliznyuk, A. A., Rendell, A. P., Allen, T. W., & Chung, S. H. (2001). The potassium ion channel: Comparison of linear scaling semiempirical and molecular mechanics representations of the electrostatic potential. *Journal of Physical Chemistry B*, *105*(50), 12674–12679.

Borgis, D., & Staib, A. (1995). A semiempirical quantum polarization model for water. *Chemical Physics Letters*, *238*(1–3), 187–192.

Bouldin, C., Sims, J., Hung, H., Rehr, J. J., & Ankudinov, A. L. (2001). Rapid calculation of X-ray absorption near edge structure using parallel computation. *X-Ray Spectrometry*, *30*(6), 431–434.

Britt, R. D., Campbell, K. A., Peloquin, J. M., Gilchrist, M. L., Aznar, C. P., Dicus, M. M., … Messinger, J. (2004). Recent pulsed EPR studies of the photosystem II oxygen-evolving complex: Implications as to water oxidation mechanisms. *Biochimica et Biophysica Acta*, *1655*, 158–171.

Brooks, B. R., Bruccoleri, R. E., Olafson, B. D., States, D. J., Swaminathan, S., & Karplus, M. (1983). Charmm—A program for macromolecular energy, minimization, and dynamics calculations. *Journal of Computational Chemistry*, *4*(2), 187–217.

Burant, J. C., Scuseria, G. E., & Frisch, M. J. (1996). A linear scaling method for Hartree-Fock exchange calculations of large molecules. *Journal of Chemical Physics*, *105*(19), 8969–8972.

Burnham, C. J., & Xantheas, S. S. (2002). Development of transferable interaction models for water. III. Reparametrization of an all-atom polarizable rigid model (TTM2-R) from first principles. *Journal of Chemical Physics*, *116*(4), 1500–1510.

Cao, J., & Berne, B. J. (1992). Many-body dispersion forces of polarizable clusters and liquids. *Journal of Chemical Physics*, *97*(11), 8628–8636.

Chen, W., & Gordon, M. S. (1996). Energy decomposition analyses for many-body interaction and applications to water complexes. *Journal of Physical Chemistry*, *100*(34), 14316–14328.

Chen, X. H., Zhang, D. W., & Zhang, J. Z. H. (2004). Fractionation of peptide with disulfide bond for quantum mechanical calculation of interaction energy with molecules. *Journal of Chemical Physics*, *120*(2), 839–844.

Cho, A. E., Guallar, V., Berne, B. J., & Friesner, R. (2005). Importance of accurate charges in molecular docking: Quantum mechanical/molecular mechanical (QM/MM) approach. *Journal of Computational Chemistry*, *26*(9), 915–931.

Chung, L. W., Hirao, H., Li, X., & Morokuma, K. (2012). The ONIOM method: Its foundation and applications to metalloenzymes and photobiology. *Wiley Interdisciplinary Reviews: Computational Molecular Science*, *2*(2), 327–350. http://dx.doi.org/10.1002/wcms.85.

Collins, M. A., Cvitkovic, M. W., & Bettens, R. P. A. (2014). The combined fragmentation and systematic molecular fragmentation methods. *Accounts of Chemical Research*, *47*(9), 2776–2785.

Cornell, W. D., Cieplak, P., Bayly, C. I., Gould, I. R., Merz, K. M., Ferguson, D. M., … Kollman, P. A. (1995). A 2nd generation force-field for the simulation of proteins, nucleic-acids, and organic-molecules. *Journal of the American Chemical Society*, *117*(19), 5179–5197.

Corongiu, G. (1992). Molecular-dynamics simulation for liquid water using a polarizable and flexible potential. *International Journal of Quantum Chemistry*, *42*(5), 1209–1235.

Daniels, A. D., & Scuseria, G. E. (1999). What is the best alternative to diagonalization of the Hamiltonian in large scale semiempirical calculations? *Journal of Chemical Physics*, *110*(3), 1321–1328.

Dapprich, S., Komaromi, I., Byun, K. S., Morokuma, K., & Frisch, M. J. (1999). A new ONIOM implementation in Gaussian 98. Part I. The calculation of energies, gradients, vibrational frequencies and electric field derivatives. *Journal of Molecular Structure*, *461*, 1–21.

Das, D., Eurenius, K. P., Billings, E. M., Sherwood, P., Chatfield, D. C., Hodoscek, M., & Brooks, B. R. (2002). Optimization of quantum mechanical molecular mechanical partitioning schemes: Gaussian delocalization of molecular mechanical charges and the double link atom method. *Journal of Chemical Physics*, *117*(23), 10534–10547.

Dau, H., Grundmeier, A., Loja, P., & Haumann, M. (2008). On the structure of the manganese complex of photosystem II: Extended-range EXAFS data and specific atomic-resolution models for four S-states. *Philosophical Transactions of the Royal Society, B: Biological Sciences*, *363*(1494), 1237–1243. http://dx.doi.org/10.1098/Rstb.2007.2220.

Dau, H., & Haumann, M. (2008). The manganese complex of photosystem II in its reaction cycle—Basic framework and possible realization at the atomic level. *Coordination Chemistry Reviews*, *252*(3–4), 273–295. http://dx.doi.org/10.1016/J.Ccr.2007.09.001.

Davis, K. M., & Pushkar, Y. (2015). Structure of the oxygen evolving complex of Photosystem II at room temperature. *The Journal of Physical Chemistry. B*, *119*(8), 3492–3498.

Day, P. N., Jensen, J. H., Gordon, M. S., Webb, S. P., Stevens, W. J., Krauss, M., … Cohen, D. (1996). An effective fragment method for modeling solvent effects in quantum mechanical calculations. *Journal of Chemical Physics*, *105*(5), 1968–1986.

Devries, A. H., Vanduijnen, P. T., Juffer, A. H., Rullmann, J. A. C., Dijkman, J. P., Merenga, H., & Thole, B. T. (1995). Implementation of reaction field methods in quantum-chemistry computer codes (Vol 16, Pg 37, 1995). *Journal of Computational Chemistry*, *16*(11), 1445–1446.

Dixon, S. L., & Merz, K. M. (1996). Semiempirical molecular orbital calculations with linear system size scaling. *Journal of Chemical Physics*, *104*(17), 6643–6649.

Dixon, S. L., & Merz, K. M. (1997). Fast, accurate semiempirical molecular orbital calculations for macromolecules. *Journal of Chemical Physics*, *107*(3), 879–893.

Dykstra, C. E. (1993). Electrostatic interaction potentials in molecular-force fields. *Chemical Reviews*, *93*(7), 2339–2353.

Eichler, U., Kolmel, C. M., & Sauer, J. (1997). Combining ab initio techniques with analytical potential functions for structure predictions of large systems: Method and application to crystalline silica polymorphs. *Journal of Computational Chemistry*, *18*(4), 463–477.

Ermolaeva, M. D., van der Vaart, A., & Merz, K. M. (1999). Implementation and testing of a frozen density matrix—Divide and conquer algorithm. *Journal of Physical Chemistry A*, *103*(12), 1868–1875.

Estrin, D. A., Tsoo, C., & Singer, S. J. (1991). Accurate nonlocal electron argon pseudopotential for condensed phase simulation. *Chemical Physics Letters*, *184*(5–6), 571–578.

Eurenius, K. P., Chatfield, D. C., Brooks, B. R., & Hodoscek, M. (1996). Enzyme mechanisms with hybrid quantum and molecular mechanical potentials. 1. Theoretical considerations. *International Journal of Quantum Chemistry*, *60*(6), 1189–1200.

Exner, T. E., & Mezey, P. G. (2002). *Ab initio*-quality electrostatic potentials for proteins: An application of the ADMA approach. *Journal of Physical Chemistry A*, *106*(48), 11791–11800.

Exner, T. E., & Mezey, P. G. (2003). *Ab initio* quality properties for macromolecules using the ADMA approach. *Journal of Computational Chemistry*, *24*(16), 1980–1986.

Exner, T. E., & Mezey, P. G. (2004). The field-adapted ADMA approach: Introducing point charges. *Journal of Physical Chemistry A*, *108*(19), 4301–4309.

Exner, T. E., & Mezey, P. G. (2005). Evaluation of the field-adapted ADMA approach: Absolute and relative energies of crambin and derivatives. *Physical Chemistry Chemical Physics*, 7(24), 4061–4069.

Fan, L. Y., & Ziegler, T. (1991). The influence of self-consistency on nonlocal density functional calculations. *The Journal of Chemical Physics*, *94*, 6057–6063.

Fedorov, D. G., & Kitaura, K. (2004a). The importance of three-body terms in the fragment molecular orbital method. *Journal of Chemical Physics*, *120*(15), 6832–6840.

Fedorov, D. G., & Kitaura, K. (2004b). On the accuracy of the 3-body fragment molecular orbital method (FMO) applied to density functional theory. *Chemical Physics Letters*, *389*(1–3), 129–134.

Ferre, N., & Angyan, J. G. (2002). Approximate electrostatic interaction operator for QM/MM calculations. *Chemical Physics Letters*, *356*(3–4), 331–339.

Ferreira, K. N., Iverson, T. M., Maghlaoui, K., Barber, J., & Iwata, S. (2004). Architecture of the photosynthetic oxygen-evolving center. *Science*, *303*(5665), 1831–1838.

Field, M. J. (1997). Hybrid quantum mechanical molecular mechanical fluctuating charge models for condensed phase simulations. *Molecular Physics*, *91*(5), 835–845.

Field, M. J., Bash, P. A., & Karplus, M. (1990). A combined quantum-mechanical and molecular mechanical potential for molecular-dynamics simulations. *Journal of Computational Chemistry*, *11*(6), 700–733.

Frisch, M. J., Trucks, G. W., Schlegel, H. B., Scuseria, G. E., Robb, M. A., Cheeseman, J. R., … Pople, J. A. (2004). *Gaussian 03, revision B.04 (version 03, revision B.04).* Wallingford, CT: Gaussian, Inc.

Gadre, S. R., Shirsat, R. N., & Limaye, A. C. (1994). Molecular tailoring approach for simulation of electrostatic properties. *Journal of Physical Chemistry*, *98*(37), 9165–9169.

Galstyan, A., Robertazzi, A., & Knapp, E. W. (2012). Oxygen-evolving Mn cluster in photosystem II: The protonation pattern and oxidation state in the high-resolution crystal structure. *Journal of the American Chemical Society*, *134*(17), 7442–7449. http://dx.doi.org/10.1021/ja300254n.

Gao, J. L. (1997). Toward a molecular orbital derived empirical potential for liquid simulations. *Journal of Physical Chemistry B*, *101*(4), 657–663.

Gao, J. L. (1998). A molecular-orbital derived polarization potential for liquid water. *Journal of Chemical Physics*, *109*(6), 2346–2354. http://dx.doi.org/10.1063/1.476802.

Gao, J. L., Amara, P., Alhambra, C., & Field, M. J. (1998). A generalized hybrid orbital (GHO) method for the treatment of boundary atoms in combined QM/MM calculations. *Journal of Physical Chemistry A*, *102*(24), 4714–4721.

Gao, J. L., & Xia, X. F. (1992). A priori evaluation of aqueous polarization effects through Monte-Carlo QM-MM simulations. *Science*, *258*(5082), 631–635.

Gao, A. M., Zhang, D. W., Zhang, J. Z. H., & Zhang, Y. K. (2004). An efficient linear scaling method for ab initio calculation of electron density of proteins. *Chemical Physics Letters*, *394*(4–6), 293–297.

Gascon, J. A., Leung, S. S. F., Batista, E. R., & Batista, V. S. (2006). A self-consistent space-domain decomposition method for QM/MM computations of protein electrostatic potentials. *Journal of Chemical Theory and Computation*, *2*(1), 175–186.

Gascon, J. A., Sproviero, E. M., & Batista, V. S. (2006). Computational studies of the primary phototransduction event in visual rhodopsin. *Accounts of Chemical Research*, *39*(3), 184–193.

Gascon, J. A., Sproviero, E. M., McEvoy, J. P., Brudvig, G. W., & Batista, V. S. (2008). Ligation of the C-terminus of the D1-polypeptide of photosystem II to the oxygen evolving complex of photosystem II. In J. F. Allen, E. Gautt, J. H. Golbeck, & B. Osmond (Eds.), *Photosynthesis: Energy from the sun* (pp. 363–368). New York: Springer.

Gentilucci, L., Squassabia, F., & Artali, R. (2007). Re-discussion of the importance of ionic interactions in stabilizing ligand-opioid receptor complex and in activating signal transduction. *Current Drug Targets*, *8*(1), 185–196.

Gill, M. L., Strobel, S. A., & Loria, J. P. (2006). Crystallization and characterization of the thallium form of the Oxytricha nova G-quadruplex. *Nucleic Acids Research*, *34*(16), 4506–4514.

Gkionis, K., Kruse, H., Platts, J. A., Mladek, A., Koca, J., & Sponer, J. (2014). Ion Binding to quadruplex DNA stems. Comparison of MM and QM descriptions reveals sizable polarization effects not included in contemporary simulations. *Journal of Chemical Theory and Computation*, *10*(3), 1326–1340.

Gordon, M. S., Freitag, M. A., Bandyopadhyay, P., Jensen, J. H., Kairys, V., & Stevens, W. J. (2001). The effective fragment potential method: A QM-based MM approach to modeling environmental effects in chemistry. *Journal of Physical Chemistry A*, *105*(2), 293–307.

Grater, F., Schwarzl, S. M., Dejaegere, A., Fischer, S., & Smith, J. C. (2005). Protein/ligand binding free energies calculated with quantum mechanics/molecular mechanics. *Journal of Physical Chemistry B*, *109*(20), 10474–10483.

Green, D. F., Dennis, A. T., Fam, P. S., Tidor, B., & Jasanoff, A. (2006). Rational design of new binding specificity by simultaneous mutagenesis of calmodulin and a target peptide. *Biochemistry*, *45*(41), 12547–12559.

Greengard, L., & Rokhlin, V. (1987). A fast algorithm for particle simulations. *Journal of Computational Physics*, *73*(2), 325–348.

Haider, S., Parkinson, G. N., & Neidle, S. (2002). Crystal structure of the potassium form of an Oxytricha nova G-quadruplex. *Journal of Molecular Biology*, *320*(2), 189–200.

Haider, S. M., Parkinson, G. N., & Neidle, S. (2003). Structure of a G-quadruplex-ligand complex. *Journal of Molecular Biology*, *326*(1), 117–125.

Halgren, T. A., & Damm, W. (2001). Polarizable force fields. *Current Opinion in Structural Biology*, *11*(2), 236–242.

Haumann, M., Muller, C., Liebisch, P., Iuzzolino, L., Dittmer, J., Grabolle, M., … Dau, H. (2005a). Structural and oxidation state changes of the photosystem II manganese complex in four transitions of the water oxidation cycle (S0 - > S1, S1 - > S2, S2 - > S3, and S3,S4 - > S0) characterized by X-ray absorption spectroscopy at 20 K and room temperature. *Biochemistry*, *44*(6), 1894–1908.

Hillier, W., & Wydrzynski, T. (2004). Substrate water interactions within the photosystem II oxygen evolving complex. *Physical Chemistry Chemical Physics*, *6*(20), 4882–4889.

Hillier, W., & Wydrzynski, T. (2008). O-18-water exchange in photosystem II: Substrate binding and intermediates of the water splitting cycle. *Coordination Chemistry Reviews*, *252*(3–4), 306–317. http://dx.doi.org/10.1016/J.Ccr.2007.09.004.

Ho, J., Newcomer, M. B., Ragain, C. M., Gascon, J. A., Batista, E. R., Loria, J. P., & Batista, V. S. (2014). MoD-QM/MM structural refinement method: Characterization of hydrogen bonding in the Oxytricha nova G-Quadruplex. *Journal of Chemical Theory and Computation*, *10*(11), 5125–5135.

Houjou, H., Inoue, Y., & Sakurai, M. (2001). Study of the opsin shift of bacteriorhodopsin: Insight from QM/MM calculations with electronic polarization effects of the protein environment. *Journal of Physical Chemistry B*, *105*(4), 867–879.

Huang, J., Lopes, P. E. M., Roux, B., & MacKerell, A. D. (2014). Recent advances in polarizable force fields for macromolecules: Microsecond simulations of proteins using the classical drude oscillator model. *Journal of Physical Chemistry Letters*, *5*(18), 3144–3150. http://dx.doi.org/10.1021/jz501315h.

Humbel, S., Sieber, S., & Morokuma, K. (1996). The IMOMO method: Integration of different levels of molecular orbital approximations for geometry optimization of large systems: Test for n-butane conformation and SN2 reaction: RCl + Cl-. *The Journal of Chemical Physics*, *105*(5), 1959–1967.

Hurley, J. H. (2006). Membrane binding domains. *Biochimica et Biophysica Acta*, *1761*(8), 805–811.

Ilan, B., Tajkhorshid, E., Schulten, K., & Voth, G. A. (2004). The mechanism of proton exclusion in aquaporin channels. *Proteins: Structure, Function, and Bioinformatics*, *55*(2), 223–228.

Illingworth, C. J. R., Gooding, S. R., Winn, P. J., Jones, G. A., Ferenczy, G. G., & Reynolds, C. A. (2006). Classical polarization in hybrid QM/MM methods. *Journal of Physical Chemistry A*, *110*(20), 6487–6497.

Kitaura, K., Ikeo, E., Asada, T., Nakano, T., & Uebayasi, M. (1999). Fragment molecular orbital method: An approximate computational method for large molecules. *Chemical Physics Letters*, *313*(3–4), 701–706.

Kitaura, K., Sugiki, S. I., Nakano, T., Komeiji, Y., & Uebayasi, M. (2001). Fragment molecular orbital method: Analytical energy gradients. *Chemical Physics Letters*, *336*(1–2), 163–170.

Ko, C., Levine, B., Toniolo, A., Manohar, L., Olsen, S., Werner, H. J., & Martinez, T. J. (2003). *Ab initio* excited-state dynamics of the photoactive yellow protein chromophore. *Journal of the American Chemical Society*, *125*(42), 12710–12711.

Kronig, R. D. (1931). The quantum theory of dispersion in metallic conductors—II. *Proceedings of the Royal Society of London. Series A, Containing Papers of a Mathematical and Physical Character*, *133*(821), 255–265.

Kronig, R. D., & Penney, W. G. (1931). Quantum mechanics of electrons on crystal lattices. *Proceedings of the Royal Society of London. Series A, Containing Papers of a Mathematical and Physical Character*, *130*(814), 499–513.

Kurisu, G., Zhang, H. M., Smith, J. L., & Cramer, W. A. (2003). Structure of the cytochrome b(6)f complex of oxygenic photosynthesis: Tuning the cavity. *Science*, *302*(5647), 1009–1014.

Lappi, A. K., Lensink, M. F., Alanen, H. I., Salo, K. E. H., Lobell, M., Juffer, A. H., & Ruddock, L. W. (2004). A conserved arginine plays a role in the catalytic cycle of the protein disulphide isomerases. *Journal of Molecular Biology*, *335*(1), 283–295.

Lee, P. A., & Pendry, J. B. (1975). Theory of the extended X-ray absorption fine structure. *Physical Review B: Condensed Matter*, *11*(8), 2795–2811.

Lee, T. S., York, D. M., & Yang, W. T. (1996). Linear-scaling semiempirical quantum calculations for macromolecules. *Journal of Chemical Physics*, *105*(7), 2744–2750.

Li, W., & Li, S. H. (2005). A localized molecular-orbital assembler approach for Hartree-Fock calculations of large molecules. *Journal of Chemical Physics*, *122*(19), 194109.

Li, S. H., Li, W., & Fang, T. (2005). An efficient fragment-based approach for predicting the ground-state energies and structures of large molecules. *Journal of the American Chemical Society*, *127*(19), 7215–7226.

Li, X. P., Nunes, R. W., & Vanderbilt, D. (1993). Density-matrix electronic-structure method with linear system-size scaling. *Physical Review B*, *47*(16), 10891–10894.

Li, X. C., Siegbahn, P. E. M., & Ryde, U. (2015). Simulation of the isotropic EXAFS spectra for the S-2 and S-3 structures of the oxygen evolving complex in photosystem II. *Proceedings of the National Academy of Sciences of the United States of America*, *112*(13), 3979–3984. http://dx.doi.org/10.1073/pnas.1422058112.

Lin, H., & Truhlar, D. G. (2005). Redistributed charge and dipole schemes for combined quantum mechanical and molecular mechanical calculations. *Journal of Physical Chemistry A*, *109*(17), 3991–4004.

Lobaugh, J., & Voth, G. A. (1994). A path-integral study of electronic polarization and nonlinear coupling effects in condensed-phase proton-transfer reactions. *Journal of Chemical Physics*, *100*(4), 3039–3047.

Lobaugh, J., & Voth, G. A. (1996). The quantum dynamics of an excess proton in water. *Journal of Chemical Physics*, *104*(5), 2056–2069.

Luber, S., Rivalta, I., Umena, Y., Kawakami, K., Shen, J.-R., Kamiya, N., … Batista, V. S. (2011a). S_1-state model of the O_2-evolving complex of photosystem II. *Biochemistry*, *50*(29), 6308–6311. http://dx.doi.org/10.1021/bi200681q.

Luzhkov, V. B., & Aqvist, J. (2000). A computational study of ion binding and protonation states in the KcsA potassium channel. *Biochimica et Biophysica Acta, Protein Structure and Molecular Enzymology*, *1481*(2), 360–370.

Maple, J. R., Cao, Y. X., Damm, W. G., Halgren, T. A., Kaminski, G. A., Zhang, L. Y., & Friesner, R. A. (2005). A polarizable force field and continuum solvation methodology for modeling of protein-ligand interactions. *Journal of Chemical Theory and Computation*, *1*(4), 694–715.

Maseras, F., & Morokuma, K. (1995). Imomm—A new integrated *ab-initio* plus molecular mechanics geometry optimization scheme of equilibrium structures and transition-states. *Journal of Computational Chemistry*, *16*(9), 1170–1179.

Mayhall, N. J., & Raghavachari, K. (2011). Molecules-in-molecules: An extrapolated fragment-based approach for accurate calculations on large molecules and materials. *Journal of Chemical Theory and Computation*, 7(5), 1336–1343. http://dx.doi.org/10.1021/ct200033b.

Mayhall, N. J., & Raghavachari, K. (2012). Many-overlapping-body (MOB) expansion: A generalized many body expansion for nondisjoint monomers in molecular fragmentation calculations of covalent molecules. *Journal of Chemical Theory and Computation*, *8*(8), 2669–2675. http://dx.doi.org/10.1021/ct300366e.

Mei, Y., Zhang, D. W., & Zhang, J. Z. H. (2005). New method for direct linear-scaling calculation of electron density of proteins. *Journal of Physical Chemistry A*, *109*(1), 2–5.

Menikarachchi, L. C., & Gascon, J. A. (2008). Optimization of cutting schemes for the evaluation of molecular electrostatic potentials in proteins via moving-domain QM/MM. *Journal of Molecular Modeling*, *14*(6), 479–487.

Mulgrew-Nesbitt, A., Diraviyam, K., Wang, J. Y., Singh, S., Murray, P., Li, Z. H., … Murray, D. (2006). The role of electrostatics in protein-membrane interactions. *Biochimica et Biophysica Acta, Molecular and Cell Biology of Lipids*, *1761*(8), 812–826.

Murphy, R. B., Philipp, D. M., & Friesner, R. A. (2000a). Frozen orbital QM/MM methods for density functional theory. *Chemical Physics Letters*, *321*(1–2), 113–120.

Murphy, R. B., Philipp, D. M., & Friesner, R. A. (2000b). A mixed quantum mechanics/molecular mechanics (QM/MM) method for large-scale modeling of chemistry in protein environments. *Journal of Computational Chemistry*, *21*(16), 1442–1457.

Nakano, T., Kaminuma, T., Sato, T., Akiyama, Y., Uebayasi, M., & Kitaura, K. (2000). Fragment molecular orbital method: Application to polypeptides. *Chemical Physics Letters*, *318*(6), 614–618.

Nakano, T., Kaminuma, T., Sato, T., Fukuzawa, K., Akiyama, Y., Uebayasi, M., & Kitaura, K. (2002). Fragment molecular orbital method: Use of approximate electrostatic potential. *Chemical Physics Letters*, *351*(5–6), 475–480.

New, M. H., & Berne, B. J. (1995). Molecular-dynamics calculation of the effect of solvent polarizability on the hydrophobic interaction. *Journal of the American Chemical Society*, *117*(27), 7172–7179.

Newville, M. (2001). IFEFFIT: Interactive XAFS analysis and FEFF fitting. *Journal of Synchrotron Radiation*, *8*, 322–324. http://dx.doi.org/10.1107/S0909049500016964.

Noodleman, L. (1981). Valence bond description of anti-ferromagnetic coupling in transition-metal dimers. *The Journal of Chemical Physics*, *74*, 5737–5743.

Noodleman, L., & Case, D. A. (1992). Density functional theory of spin polarization and spin coupling in iron-sulfur clusters. *Advances in Inorganic Chemistry*, *38*, 423–470.

Noodleman, L., & Davidson, E. R. (1986). Ligand spin polarization and antiferromagnetic coupling in transition-metal dimers. *Chemical Physics*, *109*, 131–143.

Noodleman, L., Peng, C. Y., Case, D. A., & Mouesca, J. M. (1995). Orbital interactions, electron delocalization and spin coupling in iron-sulfur clusters. *Coordination Chemistry Reviews*, *144*, 199–244.

Norel, R., Sheinerman, F., Petrey, D., & Honig, B. (2001). Electrostatic contributions to protein-protein interactions: Fast energetic filters for docking and their physical basis. *Protein Science*, *10*(11), 2147–2161.

Okamura, M. Y., & Feher, G. (1992). Proton-transfer in reaction centers from photosynthetic bacteria. *Annual Review of Biochemistry*, *61*, 861–896.

Pal, R., Negre, C. F. A., Vogt, L., Pokhrel, R., Ertem, M. Z., Brudvig, G. W., & Batista, V. S. (2013). S_0-state model of the oxygen-evolving complex of photosystem II. *Biochemistry*, *52*(44), 7703–7706. http://dx.doi.org/10.1021/bi401214v.

Palmo, K., Mannfors, B., Mirkin, N. G., & Krimm, S. (2003). Potential energy functions: From consistent force fields to spectroscopically determined polarizable force fields. *Biopolymers*, *68*(3), 383–394.

Pantazis, D. A., Ames, W., Cox, N., Lubitz, W., & Neese, F. (2012). Two interconvertible structures that explain the spectroscopic properties of the oxygen-evolving complex of photosystem II in the S_2 state. *Angewandte Chemie, International Edition*, *51*(39), 9935–9940. http://dx.doi.org/10.1002/anie.201204705.

Parr, R. G., & Yang, W. (1989). *In density-functional theory of atoms and molecules*. Oxford: Oxford University Press.

Philipp, D. M., & Friesner, R. A. (1999). Mixed ab initio QM/MM modeling using frozen orbitals and tests with alanine dipeptide and tetrapeptide. *Journal of Computational Chemistry*, *20*(14), 1468–1494.

Popovic, D. M., & Stuchebrukhov, A. A. (2004). Electrostatic study of the proton pumping mechanism in bovine heart cytochrome c oxidase. *Journal of the American Chemical Society*, *126*(6), 1858–1871.

Rappe, A. K., & Goddard, W. A. (1991). Charge equilibration for molecular-dynamics simulations. *Journal of Physical Chemistry*, *95*(8), 3358–3363.

Ren, P. Y., & Ponder, J. W. (2003). Polarizable atomic multipole water model for molecular mechanics simulation. *Journal of Physical Chemistry B*, *107*(24), 5933–5947.

Reuter, N., Dejaegere, A., Maigret, B., & Karplus, M. (2000). Frontier bonds in QM/MM methods: A comparison of different approaches. *Journal of Physical Chemistry A*, *104*(8), 1720–1735.

Rick, S. W., & Berne, B. J. (1996). Dynamical fluctuating charge force fields: The aqueous solvation of amides. *Journal of the American Chemical Society*, *118*(3), 672–679.

Rick, S. W., Stuart, S. J., Bader, J. S., & Berne, B. J. (1995). Fluctuating charge force-fields for aqueous-solutions. *Journal of Molecular Liquids*, *65–6*, 31–40.

Rick, S. W., Stuart, S. J., & Berne, B. J. (1994). Dynamical fluctuating charge force-fields—Application to liquid water. *Journal of Chemical Physics*, *101*(7), 6141–6156.

Saebo, S., & Pulay, P. (1993). Local treatment of electron correlation. *Annual Review of Physical Chemistry*, *44*, 213–236.

Saha, A., & Raghavachari, K. (2015). Analysis of different fragmentation strategies on a variety of large peptides: Implementation of a low level of theory in fragment-based methods can be a crucial factor. *Journal of Chemical Theory and Computation*, *11*(5), 2012–2023. http://dx.doi.org/10.1021/ct501045s.

Sandberg, D. J., Rudnitskaya, A. N., & Gascón, J. A. (2012). QM/MM prediction of the stark shift in the active site of a protein. *Journal of Chemical Theory and Computation*, *8*(8), 2817–2823.

Sayers, D. E., Stern, E. A., & Lytle, F. W. (1971). New technique for investigating non-crystalline structures—Fourier analysis of extended X-ray—Absorption fine structure. *Physical Review Letters*, *27*(18), 1204–1207.

Schlegel, H. B. (1987a). Optimization of equilibrium geometries and transition structures. *Advances in Chemical Physics*, *67*, 249–285.

Schmidt, M. W., Baldridge, K. K., Boatz, J. A., Elbert, S. T., Gordon, M. S., Jensen, J. H., … Montgomery, J. A. (1993). General atomic and molecular electronic-structure system. *Journal of Computational Chemistry*, *14*(11), 1347–1363.

Schwegler, E., & Challacombe, M. (1996). Linear scaling computation of the Hartree-Fock exchange matrix. *Journal of Chemical Physics*, *105*(7), 2726–2734.

Schworer, M., Breitenfeld, B., Troster, P., Bauer, S., Lorenzen, K., Tavan, P., & Mathias, G. (2013). Coupling density functional theory to polarizable force fields for efficient and accurate Hamiltonian molecular dynamics simulations. *Journal of Chemical Physics*. *138*(24). http://dx.doi.org/10.1063/1.4811292. Artn 244103.

Senn, H. M., & Thiel, W. (2009). QM/MM methods for biomolecular systems. *Angewandte Chemie, International Edition*, *48*(7), 1198–1229.

Sham, Y. Y., Muegge, I., & Warshel, A. (1998). Effect of protein relaxation on charge-charge interaction and dielectric constants in protein. *Biophysical Journal*, *74*(4), 1744–1753.

Sham, Y. Y., Muegge, I., & Warshel, A. (1999). Simulating proton translocations in proteins: Probing proton transfer pathways in the Rhodobacter sphaeroides reaction center. *Proteins: Structure, Function, and Genetics*, *36*(4), 484–500.

Shao, Y. H., Gan, Z. T., Epifanovsky, E., Gilbert, A. T. B., Wormit, M., Kussmann, J., … Head-Gordon, M. (2015). Advances in molecular quantum chemistry contained in the Q-Chem 4 program package. *Molecular Physics*, *113*(2), 184–215. http://dx.doi.org/10.1080/00268976.2014.952696.

Sheinerman, F. B., & Honig, B. (2002). On the role of electrostatic interactions in the design of protein-protein interfaces. *Journal of Molecular Biology*, *318*(1), 161–177.

Sheinerman, F. B., Norel, R., & Honig, B. (2000). Electrostatic aspects of protein-protein interactions. *Current Opinion in Structural Biology*, *10*(2), 153–159.

Shoji, M., Isobe, H., & Yamaguchi, K. (2015a). QM/MM study of the S-2 to S-3 transition reaction in the oxygen-evolving complex of photosystem II. *Chemical Physics Letters*, *636*, 172–179. http://dx.doi.org/10.1016/j.cplett.2015.07.039.

Shoji, M., Isobe, H., Yamanaka, S., Umena, Y., Kawakami, K., Kamiya, N., … Yamaguchi, K. (2015b). Theoretical modelling of biomolecular systems I. Large-scale QM/MM calculations of hydrogen-bonding networks of the oxygen evolving complex of photosystem II. *Molecular Physics*, *113*(3–4), 359–384. http://dx.doi.org/10.1080/00268976.2014.960021.

Simonson, T., Archontis, G., & Karplus, M. (1997). Continuum treatment of long-range interactions in free energy calculations. Application to protein-ligand binding. *Journal of Physical Chemistry B*, *101*(41), 8349–8362.

Simonson, T., Archontis, G., & Karplus, M. (1999). A Poisson-Boltzmann study of charge insertion in an enzyme active site: The effect of dielectric relaxation. *Journal of Physical Chemistry B*, *103*(29), 6142–6156.

Singh, U. C., & Kollman, P. A. (1986). A combined abinitio quantum-mechanical and molecular mechanical method for carrying out simulations on complex molecular systems applications to the $Ch_3Cl + Cl^-$ exchange reaction and gas phase protonation of polyethers. *Journal of Computational Chemistry*, *7*(6), 718–730.

Song, J., Ji, C., & Zhang, J. Z. H. (2013). The critical effect of polarization on the dynamical structure of guanine quadruplex DNA. *Physical Chemistry Chemical Physics*, *15*(11), 3846–3854.

Sprik, M., & Klein, M. L. (1988). A polarizable model for water using distributed charge sites. *Journal of Chemical Physics*, *89*(12), 7556–7560.

Sproviero, E. M., Gascon, J. A., McEvoy, J. P., Brudvig, G. W., & Batista, V. S. (2006a). Characterization of synthetic oxomanganese complexes and the inorganic core of the O_2-evolving complex in photosystem—II: Evaluation of the DFT/B3LYP level of theory. *Journal of Inorganic Biochemistry*, *100*(4), 786–800.

Sproviero, E. M., Gascon, J. A., McEvoy, J. P., Brudvig, G. W., & Batista, V. S. (2006b). QM/MM models of the O_2-evolving complex of photosystem II. *Journal of Chemical Theory and Computation*, *2*(4), 1119–1134.

Sproviero, E. M., Gascon, J. A., McEvoy, J. P., Brudvig, G. W., & Batista, V. S. (2007). Structural models of the oxygen-evolving complex of photosystem II. *Current Opinion in Structural Biology*, *17*, 173–180.

Sproviero, E. M., Gascon, J. A., McEvoy, J. P., Brudvig, G. W., & Batista, V. S. (2008a). Computational insights into the O_2-evolving complex of photosystem II. *Photosynthesis Research*, *97*, 91–114.

Sproviero, E. M., Gascon, J. A., McEvoy, J. P., Brudvig, G. W., & Batista, V. S. (2008b). Computational studies of the O2-evolving complex of photosystem II and biomimetic oxomanganese complexes. *Coordination Chemistry Reviews*, *252*, 395–415.

Sproviero, E. M., Gascon, J. A., McEvoy, J. P., Brudvig, G. W., & Batista, V. S. (2008c). A model of the oxygen evolving center of photosystem II predicted by structural refinement based on EXAFS simulations. *Journal of the American Chemical Society*, *130*, 6728–6730.

Sproviero, E. M., Gascon, J. A., McEvoy, J. P., Brudvig, G. W., & Batista, V. S. (2008d). QM/MM study of the catalytic cycle of water splitting in photosystem II. *Journal of the American Chemical Society*, *130*, 3428–3442.

Stern, E. A. (1974). Theory of extended X-ray-absorption fine-structure. *Physical Review B: Condensed Matter*, *10*(8), 3027–3037.

Stern, H. A., Kaminski, G. A., Banks, J. L., Zhou, R. H., Berne, B. J., & Friesner, R. A. (1999). Fluctuating charge, polarizable dipole, and combined models: Parameterization from ab initio quantum chemistry. *Journal of Physical Chemistry B*, *103*(22), 4730–4737.

Stern, H. A., Rittner, F., Berne, B. J., & Friesner, R. A. (2001). Combined fluctuating charge and polarizable dipole models: Application to a five-site water potential function. *Journal of Chemical Physics*, *115*(5), 2237–2251.

Storer, J. W., Giesen, D. J., Cramer, C. J., & Truhlar, D. G. (1995). Class IV charge models—A new semiempirical approach in quantum-chemistry. *Journal of Computer-Aided Molecular Design*, *9*(1), 87–110.

Strain, M. C., Scuseria, G. E., & Frisch, M. J. (1996). Achieving linear scaling for the electronic quantum coulomb problem. *Science*, *271*(5245), 51–53.

Stratmann, R. E., Burant, J. C., Scuseria, G. E., & Frisch, M. J. (1997). Improving harmonic vibrational frequencies calculations in density functional theory. *Journal of Chemical Physics*, *106*(24), 10175–10183.

Stratmann, R. E., Scuseria, G. E., & Frisch, M. J. (1996). Achieving linear scaling in exchange-correlation density functional quadratures. *Chemical Physics Letters*, *257*(3–4), 213–223.

Strout, D. L., & Scuseria, G. E. (1995). A quantitative study of the scaling properties of the Hartree-Fock method. *Journal of Chemical Physics*, *102*(21), 8448–8452.

Stuart, S. J., & Berne, B. J. (1996). Effects of polarizability on the hydration of the chloride ion. *Journal of Physical Chemistry*, *100*(29), 11934–11943.

Subotnik, J. E., & Head-Gordon, M. (2005). A localized basis that allows fast and accurate second-order Moller-Plesset calculations. *The Journal of Chemical Physics*, *122*(3), 034109.

Svensson, M., Humbel, S., Froese, R. D. J., Matsubara, T., Sieber, S., & Morokuma, K. (1996). ONIOM: A multilayered integrated MO + MM method for geometry optimizations and single point energy predictions. A test for Diels-Alder reactions and $Pt(P(t\text{-}Bu)_3)_2 + H_2$ oxidative addition. *Journal of Physical Chemistry*, *100*(50), 19357–19363.

Szekeres, Z., Exner, T., & Mezey, P. G. (2005). Fuzzy fragment selection strategies, basis set dependence and HF-DFT comparisons in the applications of the ADMA method of macromolecular quantum chemistry. *International Journal of Quantum Chemistry*, *104*(6), 847–860.

Thompson, M. A. (1996). QM/MMpol: A consistent model for solute/solvent polarization. Application to the aqueous solvation and spectroscopy of formaldehyde, acetaldehyde, and acetone. *Journal of Physical Chemistry*, *100*(34), 14492–14507.

Thompson, M. A., & Schenter, G. K. (1995). Excited-states of the bacteriochlorophyll-B dimer of Rhodopseudomonas-viridis—A QM/MM study of the photosynthetic reaction-center that includes MM polarization. *Journal of Physical Chemistry*, *99*(17), 6374–6386.

Thompson, M. J., Schweizer, K. S., & Chandler, D. (1982). Quantum-theory of polarization in liquids—Exact solution of the mean spherical and related approximations. *Journal of Chemical Physics*, *76*(2), 1128–1135.

Umena, Y., Kawakami, K., Shen, J.-R., & Kamiya, N. (2011). Crystal structure of oxygen-evolving photosystem II at a resolution of 1.9 angstrom. *Nature*, *473*(7345), 55–60.

van der Kamp, M. W., & Mulholland, A. J. (2013). Combined quantum mechanics/molecular mechanics (QM/MM) methods in computational enzymology. *Biochemistry*, *52*(16), 2708–2728.

Vanommeslaeghe, K., & MacKerell, A. D. (2015). CHARMM additive and polarizable force fields for biophysics and computer-aided drug design. *Biochimica et Biophysica Acta-General Subjects*, *1850*(5), 861–871. http://dx.doi.org/10.1016/j.bbagen.2014.08.004.

Vasilyev, V., & Bliznyuk, A. (2004). Application of semiempirical quantum chemical methods as a scoring function in docking. *Theoretical Chemistry Accounts*, *112*(4), 313–317.

Versluis, L., & Ziegler, T. (1988). The determination of molecular-structures by density functional theory—The evaluation of analytical energy gradients by numerical-integration. *The Journal of Chemical Physics*, *88*, 322–328.

Vreven, T., Byun, K. S., Komaromi, I., Dapprich, S., Montgomery, J. A., Morokuma, K., & Frisch, M. J. (2006). Combining quantum mechanics methods with molecular mechanics methods in ONIOM. *Journal of Chemical Theory and Computation*, *2*(3), 815–826.

Vreven, T., Mennucci, B., da Silva, C. O., Morokuma, K., & Tomasi, J. (2001). The ONIOM-PCM method: Combining the hybrid molecular orbital method and the polarizable continuum model for solvation. Application to the geometry and properties of a merocyanine in solution. *The Journal of Chemical Physics*, *115*(1), 62–72.

Vreven, T., & Morokuma, K. (2000a). On the application of the IMOMO (integrated molecular orbital plus molecular orbital) method. *Journal of Computational Chemistry*, *21*(16), 1419–1432.

Vreven, T., & Morokuma, K. (2000b). The ONIOM (our own N-layered integrated molecular orbital plus molecular mechanics) method for the first singlet excited (S_1) state photoisomerization path of a retinal protonated Schiff base. *The Journal of Chemical Physics*, *113*(8), 2969–2975.

Vreven, T., & Morokuma, K. (2003). Investigation of the $S_0 -> S_1$ excitation in bacteriorhodopsin with the ONIOM(MO: MM) hybrid method. *Theoretical Chemistry Accounts*, *109*(3), 125–132.

Vreven, T., Morokuma, K., Farkas, O., Schlegel, H. B., & Frisch, M. J. (2003). Geometry optimization with QM/MM, ONIOM, and other combined methods. I. Micro-iterations and constraints. *Journal of Computational Chemistry*, *24*(6), 760–769.

Wang, W., Donini, O., Reyes, C. M., & Kollman, P. A. (2001). Biomolecular simulations: Recent developments in force fields, simulations of enzyme catalysis, protein-ligand, protein-protein, and protein-nucleic acid noncovalent interactions. *Annual Review of Biophysics and Biomolecular Structure*, *30*, 211–243.

Warshel, A. (1976). Bicycle-pedal model for the first step in the vision process. *Nature (London)*, *260*, 679–683.

Warshel, A. (1981). Electrostatic basis of structure-function correlation in proteins. *Accounts of Chemical Research*, *14*(9), 284–290.

Warshel, A., & Aqvist, J. (1991). Electrostatic energy and macromolecular function. *Annual Review of Biophysics and Biophysical Chemistry*, *20*, 267–298.

Warshel, A., & Levitt, M. (1976). Theoretical studies of enzymic reactions—Dielectric, electrostatic and steric stabilization of carbonium-ion in reaction of lysozyme. *Journal of Molecular Biology*, *103*(2), 227–249.

White, C. A., & Headgordon, M. (1994). Derivation and efficient implementation of the fast multipole method. *Journal of Chemical Physics*, *101*(8), 6593–6605.

White, C. A., Johnson, B. G., Gill, P. M. W., & HeadGordon, M. (1996). Linear scaling density functional calculations via the continuous fast multipole method. *Chemical Physics Letters*, *253*(3–4), 268–278.

Xie, W., Orozco, M., Truhlar, D. G., & Gao, J. (2009). X-Pol potential: An electronic structure-based force field for molecular dynamics simulation of a solvated protein in water. *Journal of Chemical Theory and Computation*, *5*(3), 459–467. http://dx.doi.org/10.1021/ct800239q.

Yang, W. T. (1991). Direct calculation of electron-density in density-functional theory. *Physical Review Letters*, *66*(11), 1438–1441.

Yang, W. T., & Lee, T. S. (1995). A density-matrix divide-and-conquer approach for electronic-structure calculations of large molecules. *Journal of Chemical Physics*, *103*(13), 5674–5678.

Yano, J., Kern, J., Sauer, K., Latimer, M. J., Pushkar, Y., Biesiadka, J., … Yachandra, V. K. (2006). Where water is oxidized to dioxygen: Structure of the photosynthetic Mn_4Ca cluster. *Science*, *314*(5800), 821–825. http://dx.doi.org/10.1126/science.1128186.

Yano, J., Pushkar, Y., Glatzel, P., Lewis, A., Sauer, K., Messinger, J., … Yachandra, V. (2005). High-resolution Mn EXAFS of the oxygen-evolving complex in photosystem II: Structural implications for the Mn_4Ca cluster. *Journal of the American Chemical Society*, *127*(43), 14974–14975.

York, D. M. (1995). A generalized formulation of electronegativity equalization from density functional theory. *International Journal of Quantum Chemistry: Quantum Chemistry Symposium*, *29*, 385–394.

York, D. M., & Yang, W. T. (1996). A chemical potential equalization method for molecular simulations. *Journal of Chemical Physics*, *104*(1), 159–172.

Yu, H. B., Hansson, T., & van Gunsteren, W. F. (2003). Development of a simple, self-consistent polarizable model for liquid water. *Journal of Chemical Physics*, *118*(1), 221–234.

Zhang, D. W., Chen, X. H., & Zhang, J. Z. H. (2003). Molecular caps for full quantum mechanical computation of peptide-water interaction energy. *Journal of Computational Chemistry*, *24*(15), 1846–1852.

Zhang, Y. K., Lee, T. S., & Yang, W. T. (1999). A pseudobond approach to combining quantum mechanical and molecular mechanical methods. *Journal of Chemical Physics*, *110*(1), 46–54.

Zhang, D. W., Xiang, Y., & Zhang, J. Z. H. (2003). New advance in computational chemistry: Full quantum mechanical ab initio computation of streptavidin-biotin interaction energy. *Journal of Physical Chemistry B*, *107*(44), 12039–12041.

Zhang, D. W., & Zhang, J. Z. H. (2003). Molecular fractionation with conjugate caps for full quantum mechanical calculation of protein-molecule interaction energy. *Journal of Chemical Physics*, *119*(7), 3599–3605.